Applied Energy 342 (2023) 121198

Contents lists available at ScienceDirect

Applied Energy

journal homepage: www.elsevier.com/locate/apenergy

Techno-economic analysis of wind-powered green hydrogen production to facilitate the decarbonization of hard-to-abate sectors: A case study on steelmaking

Francesco Superchi, Alessandro Mati, Carlo Carcasci, Alessandro Bianchini *

Università degli Studi di Firenze, Department of Industrial Engineering, Via di Santa Marta 3, 50139 Firenze, Italy

HIGHLIGHTS

- Techno economic analysis on green hydrogen from an industrial perspective.
- Levelized cost of hydrogen and green index evaluation.
- Hybrid production system using wind farms, H2 storage tanks and batteries.
- Sensitivity analysis on component and electricity prices useful for policy makers.
- Evaluation of emission reduction potential in the context of EU-27 countries.

GRAPHICAL ABSTRACT

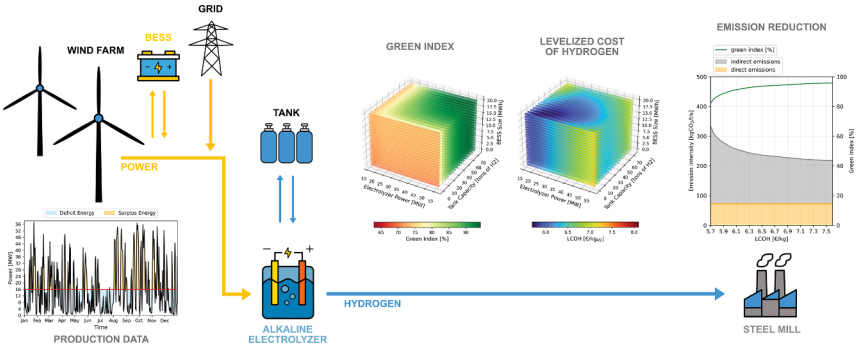

ABSTRACT

Green hydrogen is among the most promising energy vectors that may enable the decarbonization of our society. The present study addresses the decarbonization of hard-to-abate sectors via the deployment of sustainable alternatives to current technologies and processes where the complete replacement of fossil fuels is deemed not nearly immediate. In particular, the investigated case study tackles the emission reduction potential of steelmaking in the Italian industrial framework via the implementation of dedicated green hydrogen production systems to feed Hydrogen Direct Reduction process, the main alternative to the traditional polluting routes towards emissions abatement. Green hydrogen is produced via the coupling of an onshore wind farm with lithium-ion batteries, alkaline type electrolyzers and the interaction with the electricity grid. Building on a power generation dataset from a real utility-scale wind farm, techno-economic analyses are carried out for a large number of system configurations, varying components size and layout to assess its performance on the basis of two main key parameters, the levelized cost of hydrogen (LCOH) and the Green Index (GI), the latter presented for the first time in this study. The optimal system design and operation logics are investigated accounting for the necessity of providing a constant mass flow rate of H2 and thus considering the interaction with the electricity network instead of relying solely on RES surplus. In-house-developed models that account for performances degradation over time of different technologies are adapted and used for the case study. The effect of different storage technologies is evaluated via a sensitivity analysis on different components and electricity pricing strategy to understand how to favour green hydrogen penetration in the heavy industry. Furthermore, for a better comprehension and contextualization of the proposed solutions, their emission-reduction potential is quantified and presented in comparison with the current scenario of EU-27 countries. In the optimal case, the emission intensity related to the steelmaking process can be lowered to 235 kg of CO2 per ton of output steel, 88 % less than the traditional route. A higher cost of the process must be accounted, resulting in an LCOH of such solutions around 6.5 €/kg.

* Corresponding author.
E-mail address: alessandro.bianchini@unifi.it (A. Bianchini).

https://doi.org/10.1016/j.apenergy.2023.121198
Received 20 December 2022; Received in revised form 31 March 2023; Accepted 21 April 2023
Available online 29 April 2023

Nomenclature

Symbols

C	Cost [€]
E	Energy [kWh]
i	Interest rate [%]
I	Current [A]
P	Power [kW]
T	Temperature [°C]
V	Voltage [V]
η	Efficiency [%]
φ	Conversion factor [kg/MWh]

Subscripts

bess	battery
el	electrolyzer
exc	excess
grid	electrical grid
grid,hc	high cost from electrical grid
grid,lc	low cost from electrical grid
id	ideal
min	minimum
prod	produced
op	operating
purch	purchase
time,deg	time related degradation
Thermal,deg	temperature cooling related degradation
rated	rated value
req	requested
res	renewable energy sources
sell	sold
tot	total
work	actual working hours

Acronyms

AEL	Alkaline Electrolyzer
BESS	Battery Energy Storage System
BF-BOF	Blast Furnace-Basic Oxygen Furnace
CAPEX	Capital expenditures
CCUS	Carbon Capture Utilization and Storage
CF	Capacity Factor
DR	Direct Reduction
DRI	Direct Reduced Iron
EAF	Electric Arc Furnace
G	Grid
GI	Green Index
H-DR	Hydrogen-Direct Reduction
KPI	Key Performance Index
LCOE	Levelized Cost of Electricity
LCOH	Levelized Cost of Hydrogen
NG	Natural Gas
NPV	Net Present Value
O&M	Operation and Maintenance
OPEX	Operating expenditures
PEM	Proton Exchange Membrane Electrolysis
PPA	Power Purchase Agreement
PtG	Power to Gas
PUN	Prezzo Unificato Nazionale (Unified National Price)
SCADA	Supervisory Control And Data Acquisition
SF	Shaft Furnace
SOC	State Of Charge
SOH	State Of Health
SOEC	Solid Oxide Electrolysis Cell
tls	Tons of liquid steel
WF	Wind Farm

1. Introduction

The path towards a net zero emissions economy is characterized by different challenges, among which the decarbonization of the so-called "hard-to-abate" sectors, as these industries constitute about 30% of global CO_2 emissions from all sectors [1]. Conventionally speaking, this label indicates those sectors for which the transition is not straightforwardly connected to the adoption of renewables for energy production, because of either the technical characteristics of their production processes or the large costs associated to their reconversion. Heavy industry falls into this category due to the lack of readily deployable solutions in fields like cement, iron and steel, and chemicals production. These sectors can be hard to abate for many reasons, mainly due to the highly integrated and complex nature of the production processes, which often demand for extremely high temperatures (steel and aluminum) or producing emissions from non-energy sources (ammonia production). The heavy reliance on high-temperature heat for many of the processes involved in these industries constitutes a major technological limitation, as it cannot currently be sustained without generating significant greenhouse gas emissions derived from the direct use of fossil fuels. Similarly, economic constraints refer to the high cost associated with the deployment of low-carbon alternatives, which, although promising, may be prohibitively expensive or not mature enough to have a significant impact in reducing emissions in the short term as required by current policies [2]. Achieving economies of scale and reducing development costs if thus the only way to make abatement technologies become commercially viable.

1.1. Decarbonizing the steel industry

Accounting for about 8% of the global final energy demand, the iron and steel industry is responsible for 5% of CO_2 emissions in the EU and 7% globally [3], and thus constitutes a critical sector in the challenge of industry decarbonization. With an annual global production of approximately 1950 Mt of crude steel in 2021 [4] and an average output growth rate of 3.8% driven by increasing demand, the steel manufacturing industry is characterized by high energy intensity, huge production capacities and strong dependence on coal. Regarding this last point, steel production required around 15% of global coal demand in 2019 accounting for an average emission factor of 1.8 tCO_2/tls [5], with the main production technology represented by the blast furnace–basic oxygen furnace (BF-BOF) process. In such process, iron ores are reduced to pig iron in a blast furnace at temperatures above 2000 °C through a high carbon-intense reduction employing coke referred as *ironmaking* before the conversion to crude steel in the basic oxygen furnace [6]. The process-related carbon emissions are estimated around 90% of the entire production chain [7], therefore technological efforts to mitigate steelmaking environmental footprint have been attempted in recent years. Their progress is measured by the development of key projects meant to close the gap between speed of innovation and the milestones of 2030 Net Zero Scenario [8]. The two main categories of mitigation routes are broadly represented by carbon capture utilization and storage (CCUS) [9] and carbon direct avoidance technologies, with the latter encompassing options like hydrogen [10], bioenergy [11–13], direct electrification [14] and energy efficiency measures [15].

Because of its energy-intensive nature, tackling efficiency improvement and energy-saving has long been the main priority of the industry.

Efforts have been put on efficiency measures to increase the productivity of the companies and their competitiveness, and most of waste energy streams are nowadays valorized. Over the past decades, the energy intensity of steel production has been reduced by roughly 80%, from over 110 GJ consumed per ton of crude steel produced in 1970 s to the current levels of about 20 GJ/t [16]. Nevertheless, consensus exists on the fact that the technology has now reached its maturity [17] and the room for further improvement of process efficiency is small (15–20%) [18]. The primary alternative to the BF-BOF technology is represented by the shaft-type Direct Reduction-Electric Arc Furnace (DR-EAF), which relies on natural gas (NG) to convert iron ore to direct reduced iron (DRI), subsequently processing it in an EAF. The use of NG for the direct reduction operation results in a CO_2 emission profile of ~ 0.9 tons of CO_2 per ton of crude steel (tCO_2/t) which, although almost halved compared to the traditional BF-BOF route [19], makes it a process that still struggles with achieving the climate goals defined for the steelmaking industry by IEA Sustainable Development Scenario [3]. In fact, according to this study, by 2050 the average direct CO_2 emission intensity in the iron and steel sector must decline to the value of 0.6 tCO_2/t. Within this context, the global search for more sustainable pathways in steel manufacturing has been focusing lately in replacing CO_2-intensive processes with a direct reduction technology based on green hydrogen [20–22]. The basis of this approach is represented by the implementation of Hydrogen Direct Reduction (H-DR) in conjunction with the EAF (H_2-DRI-EAF process), where hydrogen is meant to replace NG as a reducing agent in the production of DRI. Considering the European scenario, several projects have been recently kicked-off across EU to explore the technical and commercial feasibility of hydrogen-based steelmaking. For example, the HYBRIT project [23] launched in Sweden is aimed at investigating hydrogen-based sponge iron production by entirely relying on fossil-free electricity. The pilot plant has been commissioned in August 2020 producing the first world's sponge iron reduced via fossil-free hydrogen gas in June 2021 [24]. The steel manufacturing corporation ArcelorMittal S.A. is developing an innovative project in Germany, aiming at the first industrial scale production and use of DRI from 100% H_2 reduction to reach the annual output of 100,000 tons of steel [25]. These examples are just a few among the noteworthy applications of hydrogen in the steel industry, and many other important industrial firms are developing similar projects, namely Tata steel, Baowu steel, Thyssenkrupp, Voestalpine etc. To better track recent developments in the sector, the reader is referred to the "Green Steel Tracker", a public database that tracks low-carbon investments in the steel industry by screening among projects associated with the pursuit of ambitious climate goals in line with the Paris Agreement targets [26].

1.2. Technologies, obstacles and prospects of green hydrogen for heavy industry decarbonization

Based on the outlined scenario, it is important to focus the attention on those hydrogen production technologies that could make it competitive on a commercial scale. Among these, green hydrogen produced via water electrolysis powered by RES is regarded as the cleanest and most appealing enabler for the development of H-DR systems, and thus the basis for energy transition of heavy industry, and particularly of the steel one.

A recent study analyzed the implementation of this process, assuming that the electricity consumption is entirely covered by the grid. This means that in addition to the operation of the EAF and ancillary processes, water electrolysis is also supplied without accounting for the presence of dedicated renewable plants [27]. Results show that, considering the current average EU grid emission factor of 295 $kgCO_2/MWh$, the emission intensity of the H_2-DRI-EAF process totals 1101 $kgCO_2/tls$.

Given that the traditional BF-BOF route reaches the value of 1688 $kgCO_2/tls$, it is worth noting that, also in this baseline case (i.e., not accounting for dedicated RES), the specific emissions of steel production could be slashed by more than 35% by means of this technology. The appropriate design and operation of dedicated green hydrogen production systems must be addressed to identify innovative strategies that can enable their uptake, hitherto considered too expensive [28]. It is well known that one of the main issues regarding green hydrogen production is the intermittent power input from renewables and its coupling with the dedicated generation system. Hydrogen request by heavy industry applications is instead usually constant over time, thus leading to possible mismatches between demand and production. One of the possible solutions to cope with this issue is the introduction of storage technologies.

When considering green hydrogen hubs, current literature generally refers to the coupling of power-to-gas (PtG) installations with fluctuating energy supply from wind and solar power stations. As for wind energy, both offshore [29]–[32] and onshore configurations [33–35] are addressed, exploring the interplay between different combinations of electrolysis technologies, storage systems and end uses both for standalone and grid-connected applications.

Focusing on electrolysis, this study considers alkaline electrolyzers as the reference technology, since to date they are recognized as the most technologically mature and reliable technology, since it has been widely deployed globally in the last decades, resulting to be the one with the largest share of installed capacity for large-scale industrial applications worldwide [36–38]. Alkaline electrolyzers present some advantages like ready market availability, non-reliance on noble metals as constitutive materials, higher longevity, and lower investment costs in comparison with the other considered typologies of electrolysis [39]. However, they also have to deal with some technical limitations like low operating pressure levels and limited values for the operational current densities (below 400 mA/cm^2) associated with the formation of potentially flammable mixtures of hydrogen and oxygen diffusing through membranes [40,41]. More importantly, they must operate in a range between 20% and 100% of the declared rated power. This feature, to some extent, negatively affects their coupling potential with unpredictable production from RES, and, as the level of detail of the analysis grows, the effects of an intermittent functioning must be considered both in the prediction of the system performance and in the modelling of the resulting wear and tear effects over the lifetime [42].

Another cornerstone for wind-fed hydrogen production is the deployment of large scale and low-cost storage, i.e., the key component able to convert the intermittent production of renewable sources into a constant hydrogen flow rate as required by steelworks applications. Currently, hydrogen storage is addressed via several technologies with main solutions being represented by physical storage, both as compressed gas or liquid, and material-based technologies [43]. While the latter is still in its development phase, and liquid storage is better suited for long haul transportation, physical storage of hydrogen in tanks via compression emerges as the optimal solution when considering large-scale production hubs like the one investigated in this study. Such an approach is not only well-developed because of the strong similarities with natural gas industry [44], but also allows for a better dynamic operation of the resource in terms of filling and releasing procedures, thus better adapting itself to the needs of complex dedicated hydrogen hubs in hard-to-abate scenarios [45].

It is then apparent that the techno-economic feasibility of utility-scale applications of green hydrogen in hard-to-abate industries must be addressed in depth to assess prospects and constraints, enabling the definition of policy-driven strategies for a successful market uptake. Lucas et al. [30] analyzed the feasibility of offshore wind-generated hydrogen in Portugal's electricity market for the WindFloat Atlantic case study, considering the variability of electricity price correlated with the respective national wind production. McDonagh et al. [32] looked at inland H_2 production fed by offshore wind power to define the optimal economic outcomes, reporting a Levelized Cost Of Hydrogen (LCOH) of 3.77 €/kg in correspondence of an LCOE of 38.1 €/MWh. Meier [46]

considered electrolysis from SOEC and PEM technologies fed with sea water on an offshore platform in Norway, analyzing techno-economic implications of hydrogen compression and transportation. Franco et al. [31] carried out energy and economic analysis of offshore productions studying the viability of different pathways for transporting hydrogen to land. Correa et al. [47] instead considered delocalized hydrogen production based on the wind resource availability in different countries, performing LCOH evaluations under various comparative scenarios that take also transportation into account. However, all these studies do not consider a specific user or the need of a constant hydrogen output, but only aim to produce H_2 in the most convenient way. When referring to hard-to-abate sectors, Nascimento da Silva et al. [48] evaluated the use of wind energy to produce hydrogen for oil refineries, defining a potential GHGs emission reduction of 22.1% for the best case scenario. Nevertheless, a gap still exists in the literature about the study of green hydrogen systems dedicated to address decarbonization in the heavy industry.

1.3. Aims of the study and novelty

The present study aims at studying the techno-economic performance of a customized hydrogen plant to convert the intermittent power production of a wind farm into a constant output of green hydrogen to be delivered to a steel industry located in Italy. Being the second largest producer in the EU-27 scenario [49] and the eleventh worldwide [50], Italy is among the nations where the adoption of hydrogen in the steelmaking sector could have a significant positive impact in terms of emissions abatement and serve as a benchmark for large economies of similar size and energy mix.

Differently from other studies which use average aggregate data for wind (namely wind distributions), here experimental data from a real utility-scale wind farm with a temporal resolution of 10 min are used. Building on such dataset, a series of 84,240 different plant configuration layouts and component sizes is simulated. Annual simulations are performed for the entire set of case studies, evaluating the influence of multiple key parameters on two major metrics, i.e. the LCOH and a newly proposed metric represented by the percentage of renewable energy used for the produced unit of hydrogen, referred to as Green Index (GI). Since the employment of electricity from both the wind farm and the power grid is considered for all cases, the GI is meant to assess the real environmental impact of the system by presenting the percentage of "green" electricity that is turned into hydrogen. To the best of authors knowledge, such an indicator has not yet been defined in literature and may represent a fundamental metric for hybrid hydrogen-generation systems.

The study goes beyond existing literature in many respects. More specifically:

a. It sheds light on the optimal system design and operation for different sizes of the wind farm and the related downstream chain in a real application scenario based on calculations from the input time-varying wind energy production.
b. It assesses how the necessity to ensure a fixed H_2 mass flow rate for the H-DR process needs affects the control logic and the management of the different energy streams instead of the reliance on RES production surplus.
c. It accounts for the implementation of realistic technologies models, also considering how the operation and degradation of components affect the system performance over time.
d. It provides a techno-economic evaluation of the entire set of tested configurations based on LCOH and GI parameters, with a focus on the effects of different storage solutions on the decarbonization rate.
e. It carries out an in-depth sensitivity analysis on different energy prices and types of incentives to investigate how explored scenarios can help new policies to foster the penetration of green hydrogen in the heavy industry.
f. It assesses the emission reduction potential of the proposed solutions and its contextualization in the EU-27 steel manufacturing scenario.
g. Ultimately, it provides a techno-economic insight relevant for short- and long-term planning of investments and policy planning. In fact, since the support of the national electricity grid appears most of the time to be unavoidable to match the industrial demand of hydrogen, efforts are aimed at quantifying and comparing the effect that incentives on fundamental components or grid electricity (both sell and purchase price) would have on the techno-economic outcomes of the system.

To address these objectives, the study is organized as follows. First, the reference case study is illustrated in Section 2, where a detailed description of the wind power generation dataset is given, followed by a discussion on the models adopted in the thermodynamic simulations. Main economic assumptions and parameters are also presented in this section. Section 3 outlines the main findings of the sensitivity analysis on the system layout. Results are presented and discussed under the light of both economic and environmental viability. Moreover, a sensitivity analysis is reported based on the projections of components prices and different market scenarios. Then, Section 4 presents and contextualizes the effective decarbonization potential of the proposed solutions in the broader European scenario. Finally, the main conclusions of the study and recommendations are outlined in the Section 5.

2. Materials and methods

2.1. Reference case study

A steel mini-mill has been considered as the reference case study to represent the final user for hydrogen production. This steelworks typology is a recently introduced kind of industrial plant implementing the EAF technology to produce continuous casting steel mainly from scrap material. More specifically, this study refers to an integrated process facility comprising the H-DR stage, as it is already commercially available [51,52]. If compared to traditional plants, mini-mills are characterized by higher operation flexibility, shorter start-up and stop times and lower production volumes, with the latter feature being key for deriving the exact amount of hydrogen to be supplied to decarbonize the process. In the present analysis, an annual yield of 100,000 tons of steel has been considered, since this order of magnitude represents a benchmark for various green hydrogen-related flagship projects currently underway at European level [53,54].

As discussed, hydrogen is necessary in this technology to substitute the coke as reducing agent in the furnace for the production process of direct reduced iron (DRI). Subsequently, the DRI is fed to the EAF together with steel scarp to be recycled, in equal shares. According to Vogl et al. [21], this process requires around 25 kg of hydrogen input per each ton of output steel, thus totaling an amount equal to 2500 ton of hydrogen per year. This corresponds approximately to a constant flow rate of 285 kg/h that must be continuously fed to the plant and thus produced via the dedicated electrolysis facility.

To satisfy this demand, an industrial-scale stack of commercial alkaline electrolyzers has been considered in modelling the system. Given that a single module can produce around 17.8 kg/h of hydrogen per MW of electric power at rated conditions, an installation of at least 16 MW of capacity is required to operate nonstop. The investigated general plant layout is presented in Fig. 1, albeit many configurations have been tested in the study also excluding some of the components in some cases. A dedicated wind farm facility provides electric energy to the electrolyzers stack when wind is available while storing overproduction in a BESS or selling it to the grid when exceeding electrolyzers rated capacity. In case wind resources are not sufficient to meet the minimum required hydrogen amount, the missing energy share is withdrawn from the national grid, thus allowing for a certain percentage of yellow hydrogen [55] to be fed to the mini-mill. Downstream the

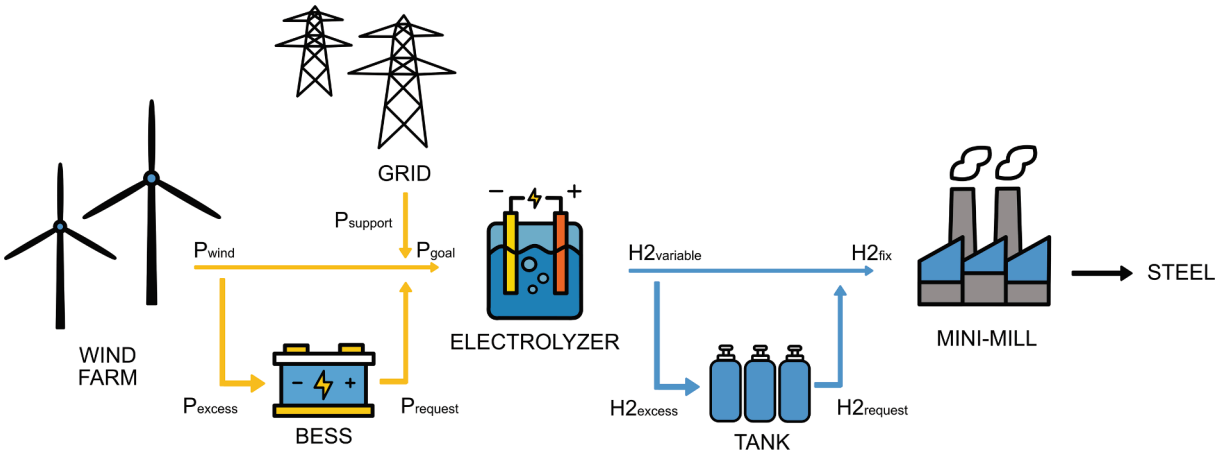

Fig. 1. Schematic diagram of the hydrogen production system. Electric power flows are represented by yellow lines, hydrogen streams by blue lines.

electrolyzers, a storage tank system can be installed to absorb any surplus of green hydrogen production. The motivation behind the presence of the two different storage solutions is to investigate and assess how to maximize the exploitation of the renewable source, allowing for higher shares of decarbonization of the process. It follows that, if tanks are present, it is reasonable to consider the installation of an electrolyzer stack with a nominal power higher than 16 MW to produce more hydrogen when wind production peaks occur. Different sizes for the portrayed system solutions are modelled, simulated and compared considering economic and environmental aspects.

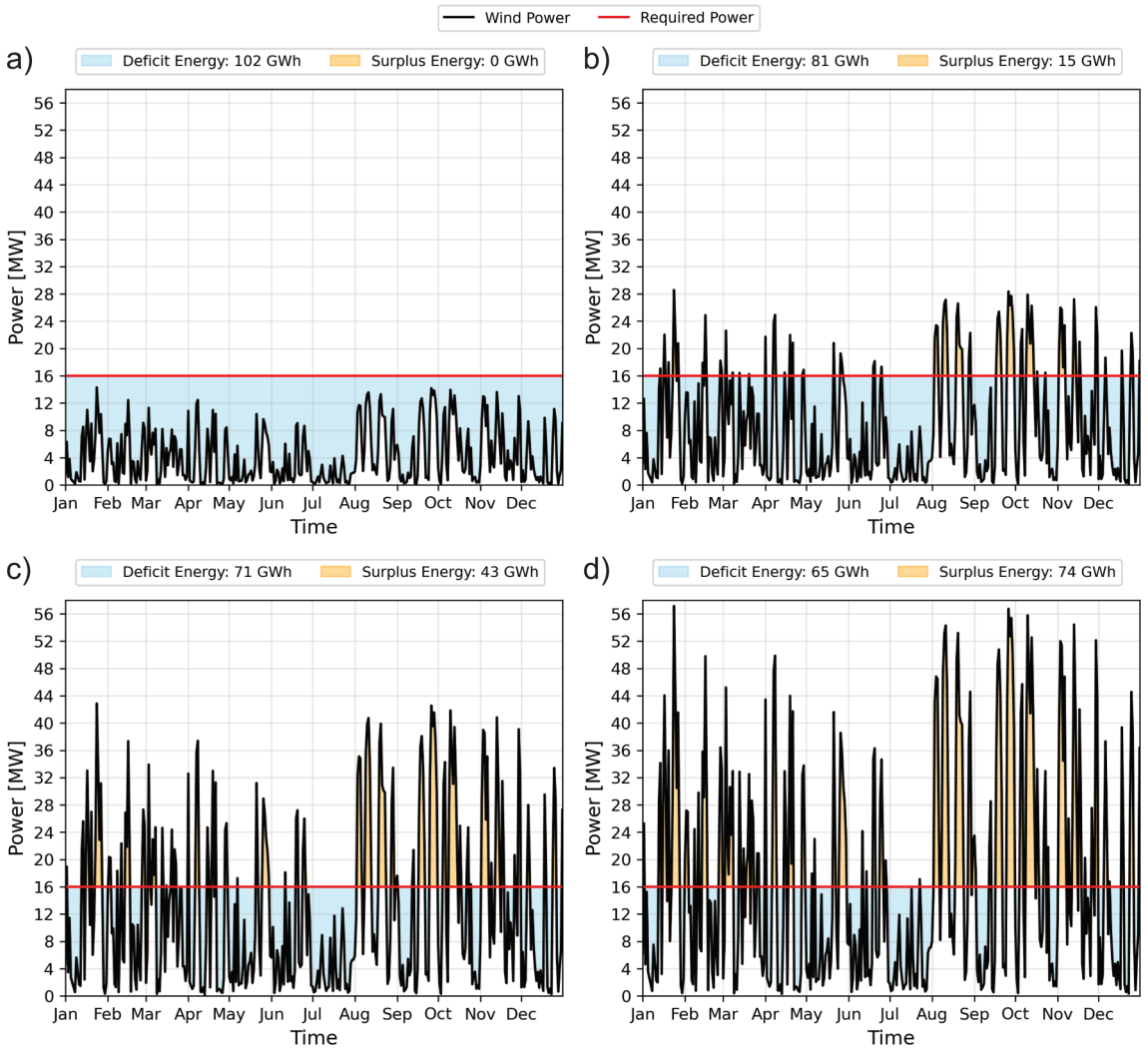

Fig. 2. Original wind farm power production scaled by 1 (a), 2 (b), 3 (c) and 4 times (d). Deficit (light blue area) and surplus (yellow area) energy quantification with respect to the constant power request form the steel mill of 16 MW (red line).

2.1.1. Wind farm

To estimate as realistically as possible the green hydrogen producibility in one year of operation, real production data of a utility scale wind farm (WF) have been fed to the simulation. Original data have been harvested from the supervisory control and data acquisition (SCADA) system of a WF located in Greece. The real production history of one year of operation with a 10-minute resolution has been kindly provided by Eunice Energy Group, the owner of the system, which is acknowledged for this. The plant is composed by six 2.3 MW onshore wind turbines; thus, the nominal power of the farm is 13.8 MW. The dataset has been analyzed and cleaned: corrupted data, measuring errors and values related to periods of maintenance, lightning and icing were removed. The data analysis showed that the capacity factor of the farm is about 30%; therefore, the number of equivalent working hours of the offshore farm corresponds to approximately 2660 h/year. Being the farm nominal power production lower than the constant power request from the electrolyzer to meet the hydrogen demand, the original dataset has been scaled up to analyze how different plant sizes would behave in this kind of application.

Fig. 2 shows the power production trend during the considered year of operation. The original power trend is scaled by 1 (a), 2 (b), 3 (c) and 4 times (d) and compared to the power request from the electrolyzer (red line). For each multiplier, the amount of deficit (blue area) and surplus energy (yellow area) that is produced with respect to the constant request from the user (red line) are shown. The original power production reported in Fig. 2 (a) lays entirely below the required threshold, meaning that, in the non-scaled scenario, a constant grid support would be required to satisfy the demand. The 2-time scaled production in Fig. 2 (b) presents several production peaks emerging above the required power line, especially during months of high production in the second half of the year. Nevertheless, the quantification of the missing energy (81 GWh) is still considerably lower than the surplus energy (16 GWh), meaning that a massive grid support would be still required. In a scenario that considers a 3-time scaled production (Fig. 2 (c)) the deficit energy drops to 71 GWh and the surplus rises to 43 GWh. The energy that must be provided by the grid decreases and the introduction of a storage system may increase the self-sufficiency degree of the system. The energy surplus becomes higher than the deficit only in the 4-time scaled scenario, corresponding to 74 GWh of surplus and 65 GWh of deficit. However, the power trend in Fig. 2 (d) shows that the surplus is not homogeneously distributed during the year. Because of this, the 100% self-sufficiency might not be reached by means of storage systems even in this scenario.

Histograms in Fig. 3 quantify the time frame in which a certain power level is maintained by the WF, again for four plant different scales: 1 (a), 2 (b), 3 (c) and 4 times (d) the original production. Power levels have been discretized into 2 MW intervals, except for the first step that ranges from 0.2 to 2 MW. The reason behind this exception is the minimum power required by the smallest considered alkaline electrolyzer module, which corresponds to 20% of its nominal power (0.2 MW for the selected technology). Since the hours in which the wind farm produces less than 0.2 MW cannot be exploited by the electrolyzer stack, those have been excluded from the counting. Hours in which the power production was lower than the power request of electrolyzers (16 MW) have been highlighted in orange. These correspond to times when external support for the operation is required (i.e., battery or grid activation).

2.2. System modelling

A dedicated simulation framework has been developed to estimate, as realistically as possible, the capabilities of the hydrogen production system for several combinations of different electrolyzers, storage systems, and wind farm scales. The 10-minute time resolution for the wind production data enables a step-by-step assessment of the behavior that the electrolyzer, the grid, the battery and the tank would follow when subjected to a control algorithm that aims to satisfy the hydrogen demand from the steel mill.

2.2.1. Electrolyzer

To assess the hydrogen production capabilities, an original electrolyzer model developed by the same authors has been used. For a detailed explanation of the model, see Superchi et al. [56]. Based on commercial devices produced by McPhy Energy, a leading company in the alkaline

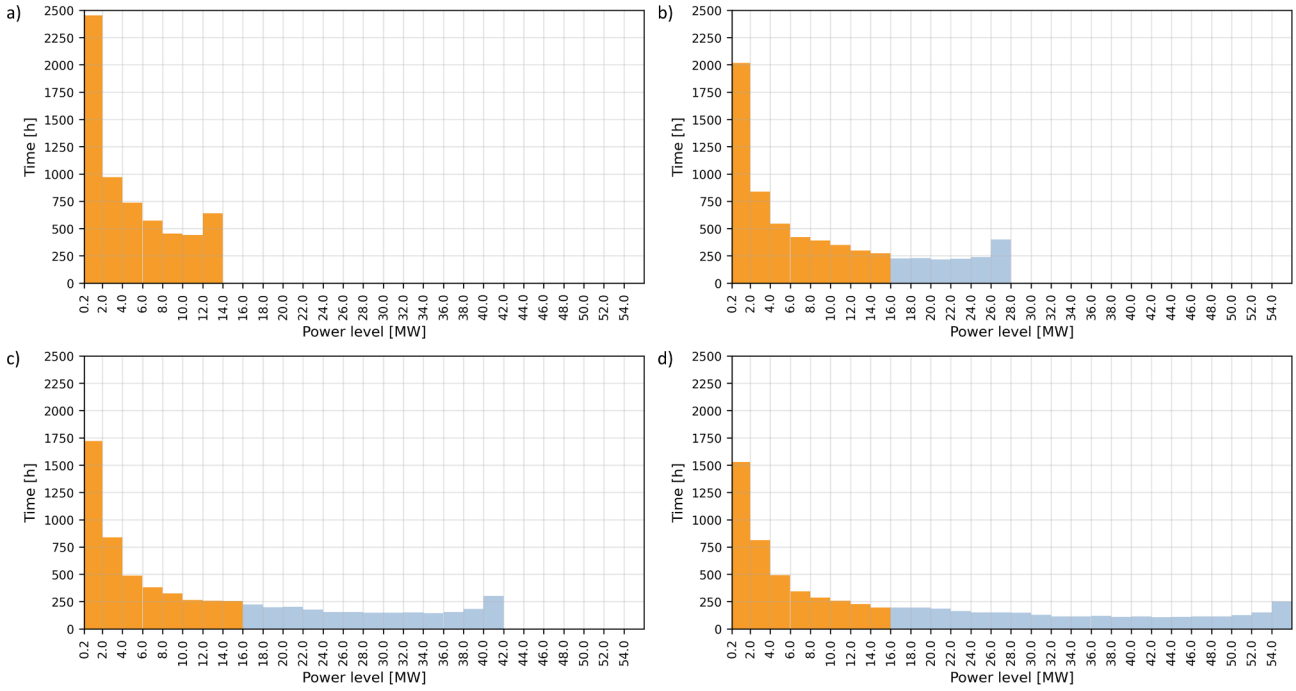

Fig. 3. Histograms of power production from wind farm scaled by 1 (a), 2 (b), 3 (c) and 4 times (d). Hours of power production lower than the required one (16 MW) are represented in orange.

electrolyzers field, the electrolyzer model has been developed with the aim to simulate a realistic operation of such a complex system. The hydrogen production capabilities of an electrolyzer change considerably when an intermittent utilization, as the one simulated in this work, undergoes. With respect to a conventional operation in which the component processes a constant power equal to its nominal value, here it works at a power level that goes from the bare minimum of 16 MW to power production peaks that may occur any time. The alkaline electrolyzer modelled here is characterized by an electric efficiency around 60%. In line with the manufacturer's datasheet, this parameter has been quantified by a power-to-gas conversion factor φ, that expresses how much hydrogen the electrolyzer it is able to produce per each MWh of input energy, equal to 18 kg/MWh. In the actual high current stack technology, time degradation causes an increase in the required voltage per working hour, while thermal degradation causes the same effect per each degree of cool down with respect to rated conditions. Considering this, Eq. (1) adjusts the operating voltage V_{op} from its ideal value considering the time effect (second term) and cooling effect (third term).

$$V_{op} = V_{id} + \Delta V_{time,deg} \cdot h_{work} + \Delta V_{Thermal,deg} \cdot (T_{rated} - T_{el}) \quad (1)$$

The operating voltage V_{op} has, in turn, an impact on the power to H_2 conversion factor φ, computed according to Eq. (2):

$$\varphi = \frac{H_{2,id}}{(I_{id} \cdot V_{op}) \cdot time} \quad (2)$$

Fig. 4 shows the trend of φ. With the same 10-minute time resolution of wind power history, the conversion efficiency of each module is updated to reach an accurate estimation of the hydrogen production: the step-by step hydrogen production is computed according to the adjusted conversion factor φ. The algorithm considers the instant availability of wind-generated electrical power, as well as the battery or grid support, to estimate the electrical energy E_{el} that can be converted to hydrogen in the given time frame. Hydrogen production is then defined by Eq. (3).

$$H_{2,prod} = \varphi \cdot E_{el} \quad (3)$$

At the end of the year-long simulation, the sum of the step-by-step H_2 output gives an accurate estimate of the yearly hydrogen production capability of the system.

2.2.2. Battery

Similarly to the electrolyzer model and based on a previous work by some of the authors [57], the BESS model simulates the real behavior of a lithium-ion battery. Among the other BESS technologies, Li-ion has been chosen for their high efficiency and resilience to cyclic operations [58]. Since this technology shows a response time in the order of milliseconds, its dynamic behavior has been neglected in this study because of the considered time step of 10 min.

Limits are imposed to the state of charge (SOC) of the battery: to avoid harmful cycles, minimum SOC is set to 15% and maximum SOC to 95%. The maximum power that the battery can absorb and release (C-rate) is limited as well, considering at least 1 h for a full charge (1C) and 30 min for a full discharge (2C). Considering those limitations and depending on the instantaneous power production from the wind farm and the power demand from the electrolyzer, the SOC of the battery is updated at each step of the simulation. Based on effects reported in the component datasheet, the battery model also considers the charging and discharging efficiency dependency on the SOC (Fig. 5). A focus on the management of the component is reported in Section 2.2.4.

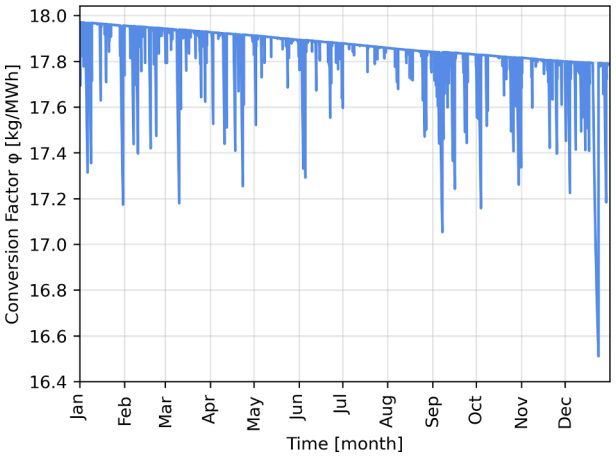

Fig. 4. Conversion factor (φ) variation in time during a year of operation of the electrolyzer.

2.2.3. Tank

A tank storage system has the function to store the hydrogen excess that may be produced by high power electrolyzers to exploit moments of power production peaks of the wind farm. For the sake of the analysis, a simplified model that tracks the quantity of H_2 that flows inside a hypothetical vessel has been introduced in the simulation. A storage pressure of 30 bar is considered, which is the same pressure level that the gas has at the output of the alkaline electrolyzer. Therefore, a further compression is not required. The model updates the SOC of this component at each time-step. In this case, for the sake of simplicity, this parameter is not limited and is allowed to go from 0 to 100%, as assumed by Mah et al. [59]. In further analyses, the tank storage sizes are quantified in terms hydrogen mass (in tons) that can be contained inside the tank at 30 bars. Fig. 6 shows the trend of the gas volume that could be stored in a configuration characterized by 37 MW electrolyzers combined with tanks able to store 117 tons of gas. Large scale modules can be used to perform a long-term storage and exploit the higher producibility of windy seasons in moments of low production or during periods of maintenance of the farm. As for the BESS, a focus on the management of the tank SOC is reported in section 2.2.4.

2.2.4. Control strategy

For each considered wind farm scale and storage capacity, the target of the hydrogen production system remains to feed the steel mill with a flow rate of 285 kg/h. To achieve this, it would be required to feed 16 MW of electrical power to the electrolyzers continuously. Due to the inherent intermittent nature of a wind farm production, it is possible to install electrolyzers with a higher nominal power to produce a hydrogen excess when an electricity production peak occurs. This hydrogen excess must be stored to be subsequently fed to the user. RES and BESS together feed the electrolyzer to produce hydrogen and, if the production exceeds the instantaneous request from the steel mill, the excess is stored inside the tanks. As previously mentioned, the SOC of the two different storage means is updated at each step of the simulation.

A parametric control strategy was applied to simulate the behavior of the system when integrating all the components. Fig. 7 reports the flow chart that schematize the control strategy to manage power and hydrogen fluxes at each considered timestep (i). The two inputs of the iteration are reported at the bottom, the current wind farm production (P_{wind}) and the hydrogen request form the steel mill ($H2_{req}$).

At the end the flow chart reports instead the two main outputs, the hydrogen produced by modules ($H2_{prod}$) and either the grid support ($G_{support}$) would be required at the beginning of the subsequent timestep or not. The battery activation always comes first: this component is the first to be charged when an excess of RES production occurs and the first to be discharged when the electrolyzer starts requiring more electricity (P_{el}) than the instantaneous production. At each timestep, the BESS control algorithm sets a target power (P_{goal}) according to the current RES production (P_{wind}) and the state of charge of the tank.

Two operational modes are considered: grid supported ($G_{support}$ = True) and islanded ($G_{support}$ = False). Grid supported mode is activated when the hydrogen contained in the tank ($H2_{tank}$) is lower than the

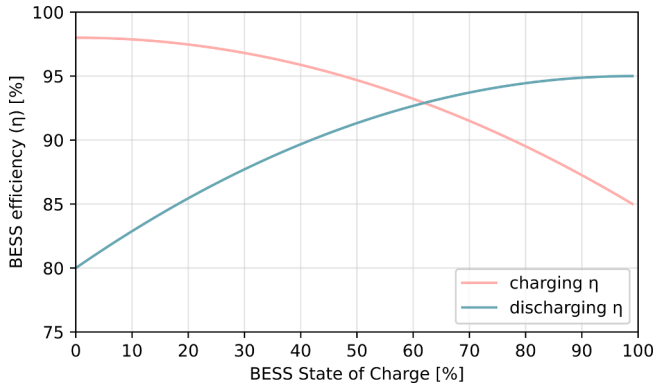

Fig. 5. Dependency of the battery charging and discharging efficiency on the state of charge.

constant request from the user ($H2_{req}$). In those moments, energy is taken from the grid (P_{grid}) to reach the target of 16 MW power to feed the electrolyzer, and the BESS is discharged only to reduce the amount of electricity that must be bought. It charges in instants of power production excess and immediately discharges when power is required. Instead, islanded mode is activated when the tank is filled and contains more hydrogen than the constant request. In these moments, the electrical grid support is not activated and the electrolyzer is powered only by the intermittent power that comes from the wind farm.

As reported before, alkaline electrolyzers requires at least 20% of their nominal power to produce hydrogen (P_{min}), hence in this mode the BESS is dedicated to keep this minimum required power level and prevent the stand-by of the modules.

Power fed to the electrolyzer (P_{el}) is converted to the equivalent amount of hydrogen that modules are able to produce, thanks to the CF update realized by the electrolyzer mode. The difference between the hydrogen produced and required will be stored inside the tanks.

2.2.5. Components SOC tracking

Fig. 8 displays the variation trend of power from the grid, battery and tank SOC during three months of the year-long simulation, for a configuration composed by 37 MW of electrolyzers, a tank capable to store 18 tons of hydrogen and a 20 MWh battery.

The red line shows that the BESS SOC, due the relatively small capacity of the component (20 MWh), shifts from the minimum to the maximum allowed values. The tank SOC line (light blue) varies in a smoother way because of the relatively high dimensions of the component (18 tons of H_2 equals to 594 MWh of energy). When both storage systems are out of charge, the grid support becomes necessary, and power (yellow line) is purchased to reach the 16 MW power level at the electrolyzer. The selected three months exemplify three possible scenarios:

a. January is an example of medium self-sufficiency. An initial SOC of 40% is hypothesized for both the BESS and the tank at the beginning of the simulation. Due to the low initial RES production, the residual energy on the battery is immediately sent to the electrolyzer and the tank is discharged in a few days. After that, the grid support is required, and power is absorbed from outside. Since the 13th day of the month, when a new period of high wind speed begun, the operation of the system was completely autonomous: BESS and tank were able to store the power and hydrogen excess and feed the steel mill without absorbing any electricity from the grid. During the last days of the month, the tank and BESS SOC shows that, during a period of very low wind power production, the storage systems combined can support the operation for around 3 days.
b. June is as an example of highly grid-dependent operation. For two thirds of the month, a massive power absorption from the grid was necessary to sustain the operation. Moments of power production peaks are mainly absorbed by the BESS. The last third of the month was characterized by a power production sufficient to maintain the autonomous operation but the tank never reaches its full capacity during this month.
c. November is an example of a highly self-sufficient operation. For almost half of the month, the tank remains full and is able, together with the BESS, to cover periods of low-RES production. Only the 1st and 25th day of the month required a grid support.

2.3. Economic parameters

When referring to the economic assessment of multi-energy systems considering the production of green hydrogen, existing literature usually relies on two main parameters, namely the Net Present Value (NPV) and the *Levelized Cost of Hydrogen* (LCOH). These indicators can be considered in conjunction [60–62] or as alternative assessment methods [63–65].

If the wind farm was not included in the considered system, the Levelized Cost Of Energy (LCOE) [66] of the renewable source should have been considered as an additional operating expense to drive the electrolysis process. This study considers a system comprising the entire farm; hence the cost of its energy is included in the calculation of the green hydrogen.

For a system that sells the hydrogen to a general market, the Payback Period (PBT) [67] would have been another important parameter for the evaluation of the techno-economic performance of the plant. PBT reflects the time needed to recover the investment, given the revenue coming from the sale of produced hydrogen. Instead, focus of this work is to assess how to satisfy the H_2 request of a specific user, thus the LCOH that the steel mill must face remains the most important parameter to evaluate.

In this paper, LCOH has been adopted as the main index for the economic analysis, such parameter is used to assess the cost of producing a unit of hydrogen for a certain time and using a certain production system as presented in several other studies concerning techno-economic analyses of hydrogen production systems (i.e., [30–32,42,47,48,68–70]). Since this methodology accounts for all the capital and operating costs of producing hydrogen, it enables the comparison of different production methods and the performance of different plant configurations. The value of this indicator is given by the point in which the actualized sum of revenues equals the actualized sum of costs: if the market price of hydrogen equals its levelized cost, the investor will recover the expenditure in the predetermined time [71].

To assess the economic feasibility of different system configurations, the LCOH is calculated as the ratio between the discounted cash flow and the discounted hydrogen output (Eq. (4)), considering a time span (t) of 20 years and an interest rate (i) of 6 %.

$$LCOH = \frac{\sum_{t=0}^{20} \frac{(CAPEX_t + OPEX_t)}{(1+i)^t}}{\sum_{t=0}^{20} \frac{H_{prod}}{(1+i)^t}} \tag{4}$$

$$CAPEX = C_{el} + C_{BESS} + C_{tank} + C_{WF} \tag{5}$$

$$OPEX = O\&M_{el} + O\&M_{BESS} + O\&M_{tank} + O\&M_{WF} + P_{purch} \cdot E_{grid} - P_{sell} \cdot E_{exc} \tag{6}$$

The Capital Expenditure (CAPEX) at time zero equals the initial investment for all the system components (Eq. (5)), it is then considered to be zero in the remaining period, except for the technologies replacement interventions.

Another important cost factor is the Operational Expenditure (OPEX) presented in Eq. (6), which considers the Operational and Maintenance costs (O&M) of each component, the cost of electricity purchased by the national grid and earnings from electricity sold to the grid.

To drive the electrolysis process, fresh water is needed as input for

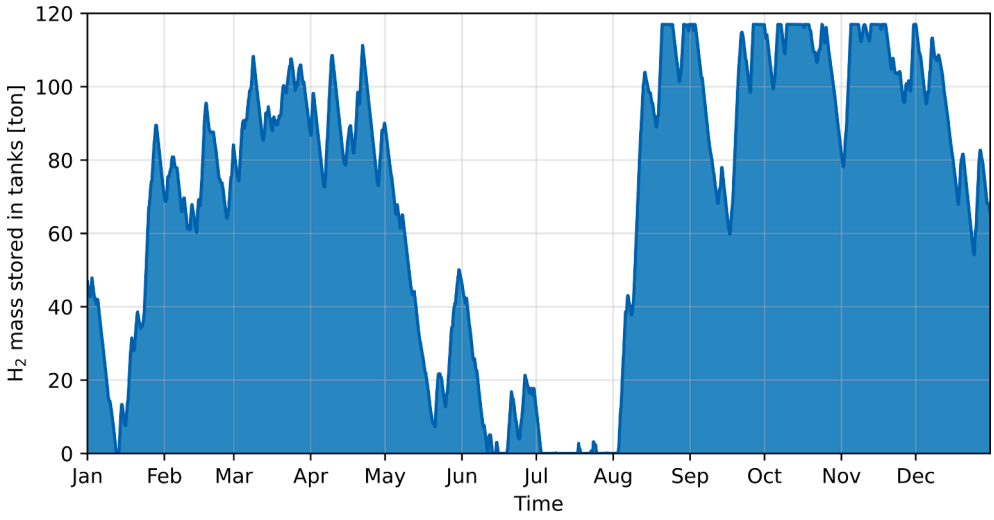

Fig. 6. Trend of the H_2 volume stored in tank storage in a configuration equipped with a 117 tons of hydrogen storage capacity.

the electrolyzer. The hydrogen production cost breakdown by Corera et al. [47] shows that water contributes to the 0.2% of the total. In this study, water cost was not directly included in the calculation but considered included in the OPEX of the electrolyzer. In addition, one valuable subproduct of the electrolysis process is oxygen [30], that may represent another earning source for the plant. This option was neglected because the selling of large quantities of O_2 is favorable only in specific markets.

Storage at high pressure, transmission and distribution costs of hydrogen were neglected as well since the analysis considers a scenario in which the H_2 is produced in close proximity to the user.

All the major economic figures considered for the calculations are reported in Table 1.

2.4. Green index

According to the act on green hydrogen by the European Commission, the rules for counting electricity from directly connected installations as fully renewables are several. Among these, hydrogen can be labelled as green if produced "during a one-hour period where the clearing price of electricity […] is lower or equal to 20 €/MWh" [79].

According to these definitions, the hydrogen produced by the system considered in this study cannot be considered fully "green" (as often erroneously claimed by similar studies), but might be partially "yellow", because the electricity sources are both the wind farm and the national grid. Bearing this in mind, a *Green Index* (GI) is defined to assess the different environmental impact of hydrogen produced with different system configurations. The GI is calculated with Eq. (7), where E_{wf} is the electricity that the wind farm produces and the electrolyzers uses, which is considered 100% green, while $E_{grid,lc}$ and $E_{grid,hc}$ are the electricity purchased by the national grid at times of low and high cost, respectively. According to the current energy mix of a country like Italy, the first is considered 100% green, while the second is yellow but can be considered 36% green [80]. E_{tot} is the sum of the three terms.

$$GI = \frac{E_{WF} + E_{grid,lc} + 0.36 \cdot E_{grid,hc}}{E_{tot}} \tag{7}$$

3. Results and discussion

This section presents the results of an in-depth parametric analysis aimed at assessing the sensitivity of techno-economic parameters, namely LCOH and GI on the variation of system configuration in terms of wind farm size, battery, and tank capacity. Market values for electricity price in the baseline scenario have been set to 70 €/MWh for sale and 150 €/MWh for purchase, respectively. Assumptions on the sale price for the excess wind energy are derived from both the global weighted average Levelized Cost Of Electricity (LCOE) of new onshore wind projects [77] and the most recent wholesale energy prices under the power purchase agreement (PPA) schemes adopted in Europe [78]. On the other hand, the selected purchase price for electricity is related to the average values of the Italian unified national price (PUN) for the two-year period 2021–2022 [76].

Table 2 reports the results of a configuration without any storage for the four wind farm sizes introduced before. Since there is no possibility to store any excess of power, an electrolyzer with a rated power of 16 MW is installed, sufficient to produce the amount of hydrogen required by the steel mill. When the power production from the wind farm is below the required 16 MW, energy is purchased from the grid. Instead, power excess during wind production peaks is entirely sold to the grid. As expected, due to the significant difference between the selling and purchase price, scenarios with a larger wind farm that increases the self-sufficiency of the plant lead to an inevitable drop in the LCOH.

The lowest LCOH that can be obtained in absence of a storage system is 5.89 €/kg, when the electrolyzer is connected to a 4-time scaled wind farm. This configuration leads to a GI of 70.29%, meaning that only 30% of the hydrogen that is fed into the steel mill is "yellow hydrogen". This value is still considerably higher than the market price of "grey" hydrogen, that currently ranges between 1 and 2 €/kg [81]. An energy storage system allows rising the GI of the hydrogen produced by the plant thank to the increasing in the degree of exploitation of wind energy. To assess economically reasonable capacity ranges for the BESS and the hydrogen tank, a preliminary and wide range analysis was performed. The two storage means were considered separately, and the aim was to evaluate the cost of reaching 100% of green hydrogen by using one technology or the other. The analysis was carried out considering a wind farm scaled by a factor of 4. Then, the LCOH figures resulting from such solutions have been computed to compare the economic performance of BESS-based solutions with tank-based solutions. Results are plotted in Fig. 9.

All BESS-based solutions consider an electrolyzer stack of 16 MW nominal power. The storage is located between the power source (wind farm) and the electrolyzer, thus there is no possibility to store an excess of hydrogen that could be produced by a larger electrolyzer. On the other hand, if one wills to exploit a tank storage system, it is necessary to increase the electrolyzer power at higher levels than the bare minimum required to meet the steel mill demand. For this reason, tank-based solutions consider electrolyzer capacities proportional to the increasing tank size.

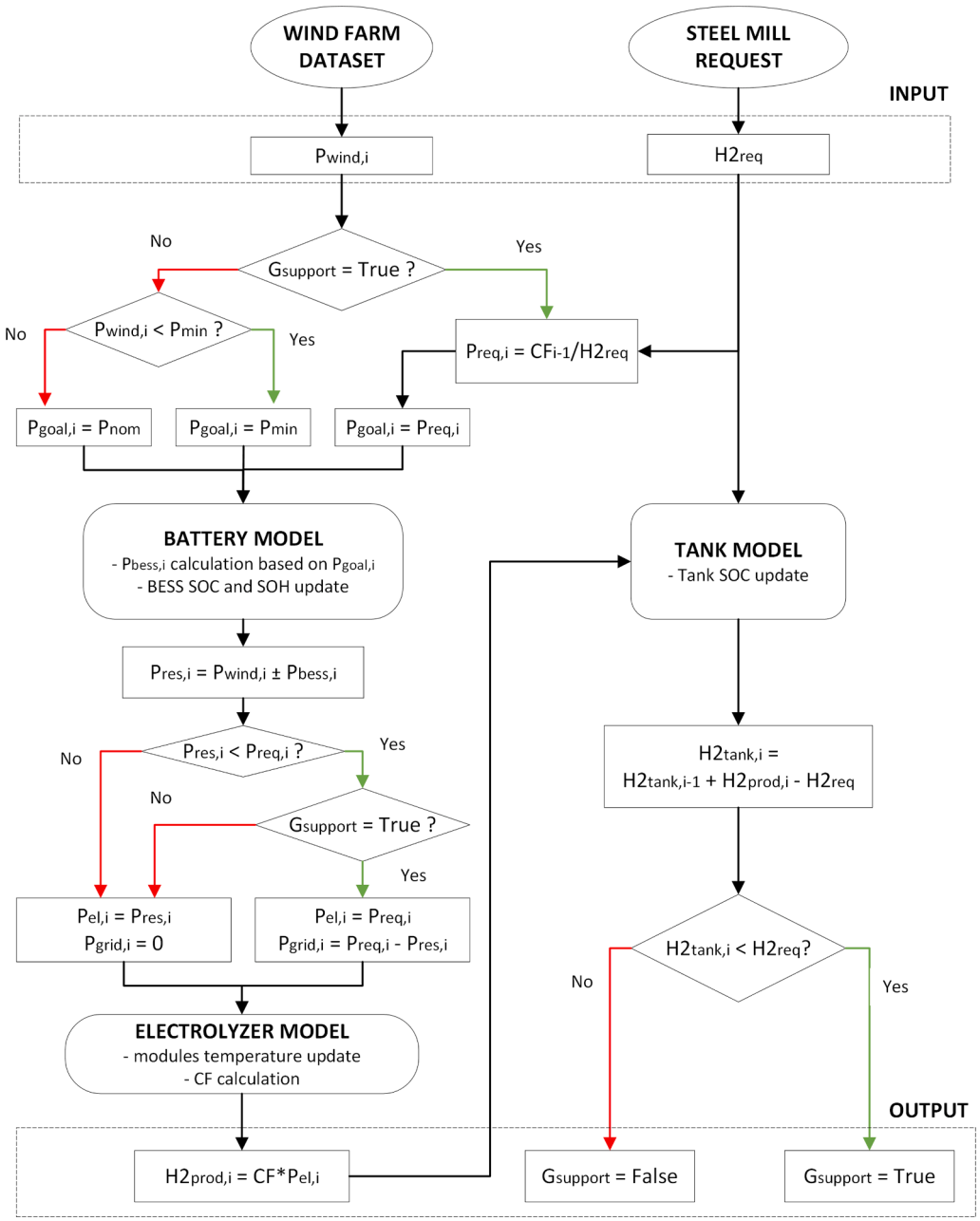

Fig. 7. Flow chart of the control strategy that manages energy and hydrogen fluxes in each considered timestep.

Results show that, when the target is to reach GIs slightly higher than that obtained by a configuration without storage systems, the optimal solution is to install a small battery. In this GI range (70–72%), a BESS allows to increase the GI without increasing the size of the electrolyzer. Indeed, when the target is to reach GIs higher than 74%, the combination of a hydrogen tank and a higher electrolyzer installed power becomes more effective. To reach high GIs, it is considerably more convenient to install high-capacity tanks with respect to high-capacity batteries.

Based on these results, the capacity range for the BESS was set to 0–20 MWh and the tank sizes goes from 0 to 117 tons of hydrogen. The main technical assumptions and the capacity range of each component considered in the parametric analysis have been summarized in Table 3.

3.1. Hydrogen tank

Fig. 10 shows the LCOH and GI trend varying the tank capacity for different sizes of the electrolyzer for systems powered by the wind farms with increasing scale factor, i.e., 2x (Fig. 10 (a)), 3x (Fig. 10 (b)) and 4x (Fig. 10 (c)). For the purposes of this analysis, only discretized intervals of 18 tons for the tank capacity have been considered in order to portray the qualitative trend of performance. An electrolytic power ranging from 16 MW up to the nominal power of the wind farm (i.e.: 28 MW for the 2x, 42 MW for the 3x and 56 MW for the 4x) was considered.

It is important to emphasize that the black line shown in the graphs relates to a configuration with no tank installed and confirms that in absence of a storage medium, an increase in electrolyzer power only produces a linear increase in the LCOH and no improvements in the GI and should therefore be avoided. On the other hand, when a tank is present, the installation of a high electrolytic capacity not only improves the GI but, in configurations with a high amount of available renewable power, it may also decrease the LCOH. A higher level of self-sufficiency, given by the possibility of exploiting power production peaks, increases the use of the renewable resource and decreases the amount of

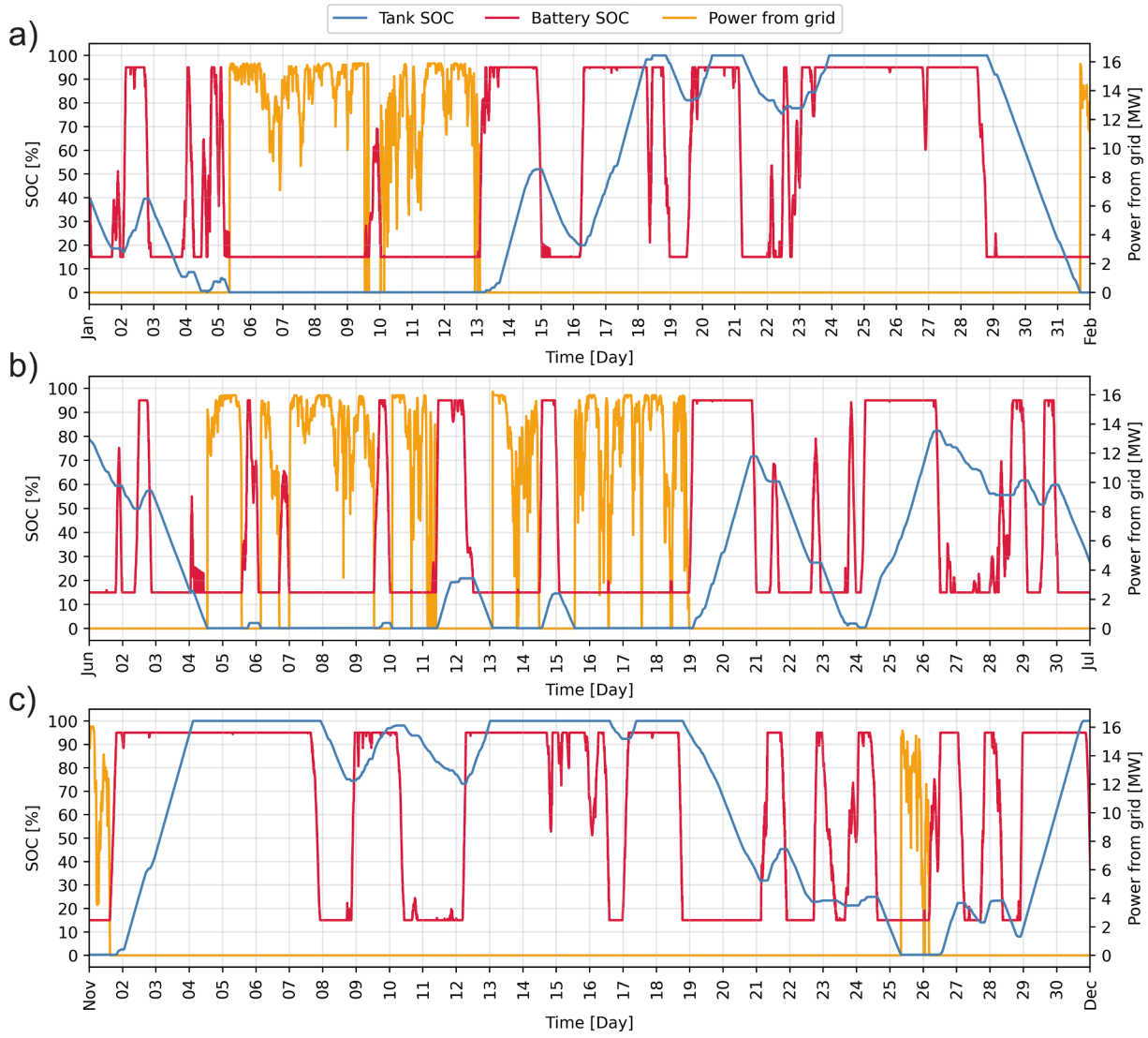

Fig. 8. Tank and BESS SOC and electrical grid power request trend during a month of operation. January (a), June (b), November (c).

electricity that must be purchased from the grid.

In configurations paired with a wind farm scaled by 2 times (Fig. 10 (a)) compared to the original dimension, the GI starts from 63% (16 MW, no tank) and reaches values around 70% (28 MW with tank). The dash dotted blue line represents the trend of the LCOH resulting from systems that utilize tanks able to store 18 tons of H_2. This line presents a minimum when paired with a 24 MW electrolyzer: a good trade-off between GI (68.75%) and LOCH (6.96 €/kg). The effect on the GI of tank sizes larger than the latter is negligible, and it only produces an increase in the LCOH: for each additional 18 tons of H_2 storage capacity, the GI gain is around 0.1%, while the LOCH increment is around 32c€/kg.

When a wind farm scaled 3 times the original size (Fig. 10 (b)) powers the system, GI starts around 68% (16 MW, no tank) and can be increased up to 87.5% (42 MW with tank). In this case, due to the high availability of cheap renewable energy, the installation of a tank can reduce the LCOH to values lower than the standard configuration with no storage means and low electrolyzer power. A tank capable to store 18 tons of H_2, paired with a 25 MW electrolyzer, results in a LOCH reduction of 7c€/kg with respect to the hydrogen cost resulting from the configuration without storage. This effect is even more pronounced in configurations powered by a wind farm 4 times the original size (Fig. 10 (c)), where the GI can be increased from 70% to almost 96% thanks to the tank storage system. This scenario brings to the lowest LCOH reachable for the discretized analysis: a 30 MW electrolyzer equipped with a tank capable to store 18 tons of H_2 results in a LOCH of 5.71 €/kg, and a GI of 83.5%. This is also the scenario that allows one to reach the highest possible GI: a 56 MW electrolyzer equipped with a 117 tons capacity H_2-tank system reaches a GI of 95.53%, but the resulting LCOH is 7.36 €/kg. Generally, presented analysis shows that, when a storage system is present, the LCOH trend varying the electrolyzer power always shows a minimum. For each tank size, there is an electrolyzer rated power that optimizes the trade-off between the higher initial investment for the storage system and the consequent electricity purchase savings. A

Table 1
Main economic parameters considered in the study.

Component	CAPEX	OPEX	Lifetime	Reference
Electrolyzer	650 €/kW	2.75% I_0 €/y	10 years	[72]
BESS	117 €/kWh	2.5% I_0 €/y	10 years	[73]
H_2 Tank (30 bar)	460 €/kg	1% I_0 €/y	20 years	[72,74]
Wind Farm	1279 €/kW	42 €/kW/y	25 years	[75]
P_{purch} grid	–	150 €/MWh	–	[76]
P_{sell} grid	–	70 €/MWh	–	[77,78]

better description of this phenomenon is reported in section 3.4.

3.2. Battery energy storage system (BESS)

Fig. 11 shows the effect that a battery storage system can have on the levelized cost of hydrogen and green index in the configurations with 16 MW electrolyzers. As pointed before, when only this kind of storage is present, electrolyzers must produce exactly the constant request from the user, and thus only 16 MW of installed power is considered. The capacity range of the BESS goes from 0 to 20 MWh. As expected, the introduction of a BESS increases the GI and, until a certain dimension, reduces the LCOH. As for the tank, the augmented self-sufficiency makes the produced gas greener and reduces the amount of electricity that must be acquired from the grid. The minimum is again given by the trade-off between purchase savings and higher initial investment. The positive effect that the storage has on the GI scales up with the size of the wind farm. The increase in GI by a 20 MWh capacity BESS is 1.92% for the smallest considered plant (2x), 2.33% in the middle case (3x) and 2.54% for the biggest one (4x). Noteworthy, the GI trend seems to flatten out with increasing BESS capacity, thus indicating that a further gain in electrical storage size would result in minor environmental returns. The increment in wind farm scale makes the minimum of the LCOH shifting towards bigger BESS sizes: 10 MWh in the 2x case, 13 MWh for the 2x and 18 MWh for the 4x.

These results prove that a relatively small BESS (compared to considered capacities for the tank) can reduce the LCOH of configurations with lower electrolytic capacities.

3.3. Combined system

The effect of the combination of the two storage systems is analyzed in this section. The three-dimensional plots presented in Fig. 12 and in Fig. 13 are meant to give a global overview on how the variation in size and the interplay of the three main components affect the technoeconomic outcomes of the system for the three different wind farm dimensions considered. Defined ranges are presented in Table 3; greater wind farm dimensions imply the simulation of a wider capacity spectrum also for the considered production and storage technologies to expand the coverage of the present analysis. The total number of different configurations tested is to 84,240 and, for each of them, a yearlong simulation has been performed leading to specific LCOH and GI results that help in the visualization and interpretation of the complexities of this analysis (given the number of variables).

Fig. 12 displays the results of the LCOH for all the tested different layouts, presented in the same scale of magnitude for a better understanding of the effects of the overall system size variation. Fig. 12 (a) is characterized by the highest LCOH figures and refers to a configuration of the wind farm scaled by 2 times. The simultaneous installation of both large tank and BESS systems when little electrolysis capacity is available has inevitably a negative impact on the metric since all the storage potential is not fully exploited. On the other hand, the lowest LCOH value of 6.75 €/kg is obtained when an electrolyzer stack of 16 MW is coupled with a BESS of 10 MWh and no other storage mean is present.

Given the poor matching between the renewable source availability and the facility needs, the grid support is frequently activated; the presence of electrical storage for the configuration with the lowest LCOH is prime indicator of the influence of the price delta between the sale and purchase of electricity, which leads to a preference for storing energy at zero cost when available.

Table 2
LCOH and GI for a system without any storage for different WF scales.

WF Scale	1x	2x	3x	4x
LCOH [€/kg]	7.66	6.78	6.29	5.89
GI [%]	53.17	62.89	67.31	70.29

When a 3-time scaled wind farm is considered (Fig. 12(b)), also components size ranges are broadened. For this case, the influence of the tank storage system begins to make its impact, allowing a minimum LCOH value of 6.17 €/kg to be reached when 24 MW of electrolyzers are connected to a 9 tons capacity tank system and no BESS is installed. Finally, values of Fig. 12(c) are representative of the largest system capacities simulated and coupled with a 4-time scaled wind farm. For the best case, higher storage capacities are paired with high power electrolyzers, higher investment costs may be better balanced by the cost reduction in hydrogen production. In fact, the LCOH index significantly decreases to a minimum value of 5.69 €/kg in the presence of a 13.5 tons capacity for the tanks and an electrolysis rated power of 28 MW without the support of any electrical storage mean.

As important as the economic assessment, the environmental score of all the combinations tested is presented in Fig. 13. Similar to the image discussed above, GI results are portrayed for the different wind farm dimensions and plotted over the same interval to display the evolution of performance as considered size ranges increase. Starting from Fig. 13(a), it is apparent that the system is under-dimensioned to achieve an acceptable GI value for the constant grid support required to meet hydrogen demand. The best outcome is obtained for 28 MW electrolyzers, 20 MWh of BESS capacity and 72 tons of tank size, accounting for a GI of 70.5%.

Fig. 13 (b) is instead useful to understand the trend for higher installed storage capacities. Configurations with high storage volumes allow a higher penetration of renewable energy generated by the wind farm, leading the 3D graph to a distinct transition to green in correspondence with the latter. For the wind farm scaled by a factor three, the highest GI is 86.35%, generated by a process layout with 42 MW of electrolyzers and 20 MWh and 72 tons capacity for BESS and tanks system, respectively. Among the many cases studied, the best possible outcome is achieved by the highest storage capacities coupled with a 56 MW electrolyzers stack, accounting for a remarkable 94.28% GI score. These results are depicted in Fig. 13(c) and show that for a wind farm four times the original size, it is possible to decarbonize the hydrogen production process nearly completely.

Fig. 14 helps to better grasp the results presented above by representing in the same graph the evolution of the two KPIs for different scales of the wind farm. While the effects of a storage capacity increase are detrimental both from an economic and an environmental point of view for the smallest wind farm, as shown in Fig. 14(a), the same does not apply for larger systems. It is interesting to observe that the family of curves tends to move progressively towards the lower right-hand side of the graphs, implying that both the parameters improve as the system size increases, LCOH declines while GI grows. Minimum values for the cost of production are found in solutions that consider the installation of storage systems: the variation in BESS size is not relevant with respect to the effects of increasing the tank system capacity, also due to the small range considered for the first technology. Fig. 14(c) allows to visualize that for the 4-time scaled wind farm, the presence of high-capacity storage tanks strongly affects the minimum value of LCOH, which, despite the higher initial investment compared to the case without storage, enables improved economic performance due to the electricity cost difference between purchase and sale prices. As previously mentioned, minimum LCOH value is 5.69 €/kg, and it occurs for a tank capacity of 13.5 tons. Larger tank sizes initially cause a significant translation towards higher GI figures, progressively decreasing their contribution thereafter when the shift becomes vertical, yielding only a significant increase in LCOH compared to a negligible gain in GI.

3.4. LCOH contributors

To understand the weight of different contributors on the final price of green hydrogen, and how this contribution varies when the storage of the electrolyzer size is increased, Fig. 15 shows the LCOH variation as a function of different cost contributors. This analysis considers a fixed

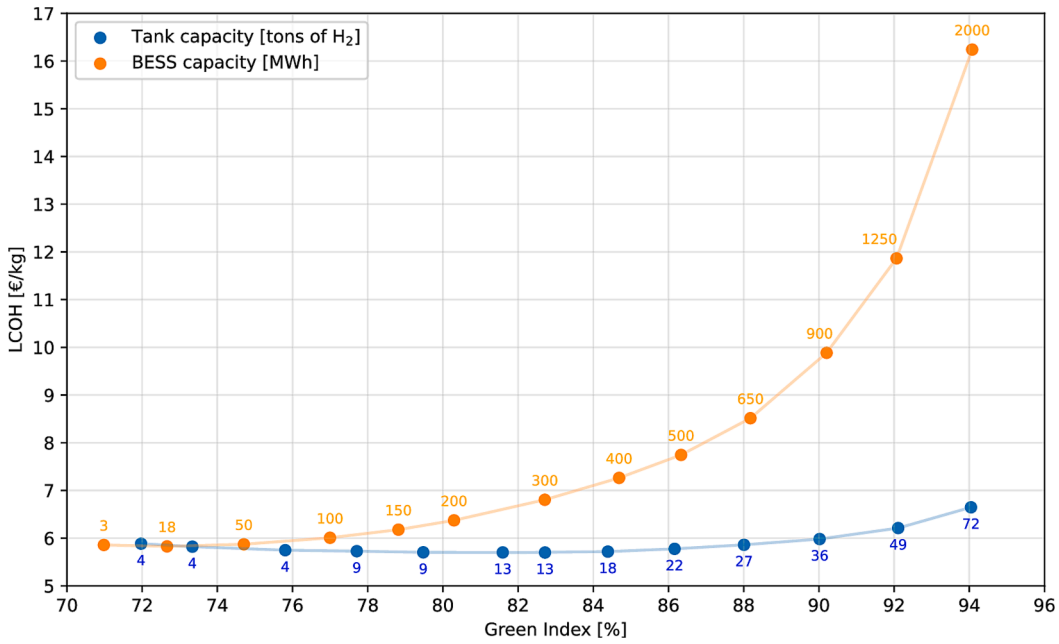

Fig. 9. Comparison of LCOH trends between BESS (orange line) and tank (blue line) supported operation to parity of Green Index (GI). Lines interpolate discrete simulations (represented by marks) and labels indicates the size of the considered storage system: MWh for BESS and tons of hydrogen for tanks.

Table 3
Technical assumptions of the main components of the system: electrolyzer, battery, H_2 tank and wind farm.

Component	Technical assumptions	Capacity range
Electrolyzer	Variable Temperature (71 °C nominal)	16–28 MW (2x)
	Variable Voltage (1.91 V initial)	16–42 MW (3x)
	18 kg/MWh	16–56 MW (4x)
Battery	15–95% SOC	0–20 MWh
	SOC dependent efficiency	
H_2 Tank	0–100% SOC	0–117 tons of H_2
	30 bar	
Wind Farm	Enercon E-82 (2.3 MW)	14 MW (1x)
	10 min time resolution data from SCADA system	28 MW (2x)
		42 MW (3x)
		56 MW (4x)

tank size of 9 tons of hydrogen and a wind farm scaled 4 times. The increment of the electrolyzer power produces a linear increase in the initial investment cost (dotted line) and, consequently, a linear increase in the operation and maintenance of the plant (dash-dotted line). On the other hand, this increment results in a drop of the electricity purchase expenditure (dashed line). This drop is not linear and flattens around a 44 MW electrolyzer: since the tank size is limited, a further increment in the electrolyzer power does not result in a correspondent increment in the system self-sufficiency.

The minimum present in the global LOCH (continuous line) corresponds to the optimal trade-off between the electricity purchase expenditure drop and the initial investment increment. If the electrolyzer power is additionally increased, the higher initial investment is not balanced by the electricity savings. The introduction of a BESS system (different line colors) reduces the LCOH when the electrolyzer power is low, but only translates in an increase when the power of this components becomes higher than 23 MW: the electricity expenditure savings become smaller and smaller, as evidenced by the reciprocal position of dashed lines.

3.5. Sensitivity analysis

This section presents the results of an economic optimization performed under different market scenarios that may present significant variations of the electricity and components prices. An increment in the market price of electricity can be produced by market fluctuations, as it is discussed below. A reduction in components prices may be given by the advancement and diffusion of such devices. Additionally, a price reduction in those two areas may be given by public incentives that aim to boost the penetration of green technologies.

The prediction of future outcomes is intrinsically characterized by high levels of uncertainty, and this influences all the factors and quantities that this sensitivity analysis considers. Hence, all displayed results are meant to give an insight into different potential evolutions of the market scenario. To address this uncertainty, the analyses consider a wide range of assumptions with the aim to cover as many probable techno-economic developments as possible and provide a comprehensive picture of their potential impact. In this context, this analysis may help the reader to understand how such subsidies would affect the optimal solution. All analyses in this section consider a wind farm scaled 4 times with respect to the original plant.

3.5.1. Price of system components

As pointed in Section 3.4, the production cost of hydrogen is influenced by several technical and economic contributions. One of the most important is the CAPEX requirement for the various components that make up the plant, i.e., wind turbines, electrolyzers, batteries and tanks. Technological improvements, new materials, new production methods and economy of scales will reduce the current costs of these components. Regarding electrolyzers, the development of new materials for electrodes and membranes and a future economy of scale in the manufacturing process could lead to a drastic drop in the production cost of the stacks. IEA foresees a cost reduction of 20% in alkaline electrolyzers because of the advent of scaled-up electrolyzers and automated production processes [82]. The Norwegian electrolyzer maker Nel declared a plan to cut the cost of their devices by 75% in a new Gigafactory that they are building [83]. According to Irena [84], the cost of hydrogen electrolyzers could fall during the next decade at similar rates to those seen in solar panels and wind turbines: minus 82% and 39%, respectively, between 2010 and 2019. The cost of lithium-ion batteries has declined by 97% between 1991 and 2018 [85]. According to IRENA [86], Li-ion batteries are still a relatively new technology, and

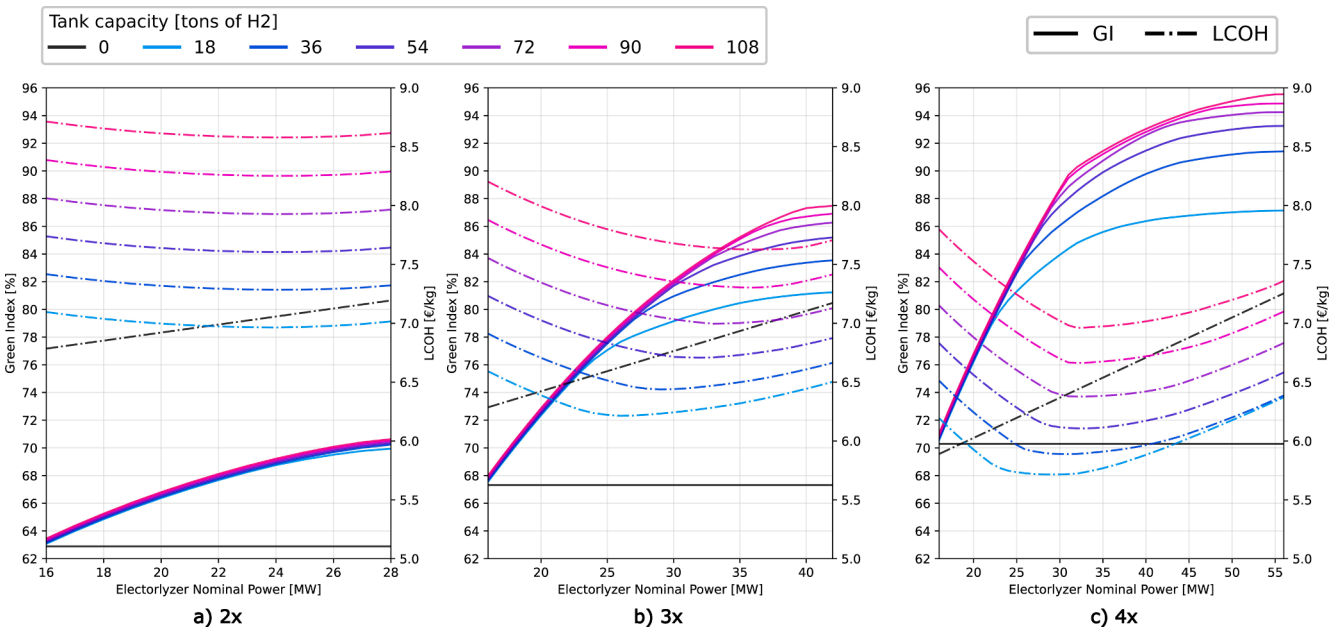

Fig. 10. LCOH (dash-dotted line) and Green Index (continuous line) trend varying tank capacity in tank supported operation for different scales (2x, 3x and 4x). Different tank sizes are represented by different colors.

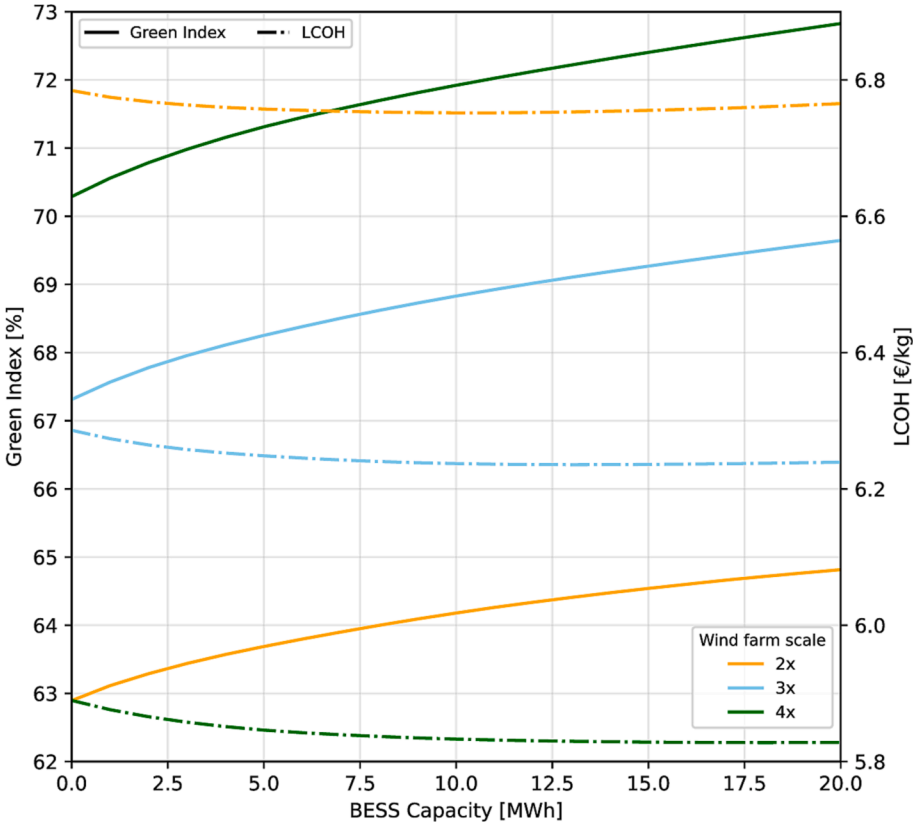

Fig. 11. LCOH (dash-dotted line) and Green Index (continuous line) trend varying battery capacity in BESS supported operation for different scales. Different wind farm scales are represented by different colors.

their potential cost reduction is large: increase in the scale of production capacity, new materials, more competitive supply chains and performance improvements are the most promising factors for a further cost reduction. BNEF forecasts a LI-ion batteries prices fall to 73 $/kWh in 2030 [87]. In line with electrolyzers and batteries, research on new materials and the growing increase on the hydrogen tanks demand could produce similar price drops even in these components. To estimate the future economic implications of market evolution on hydrogen production plants, the following sections present the effect that the components price drop could have on the final LCOH.

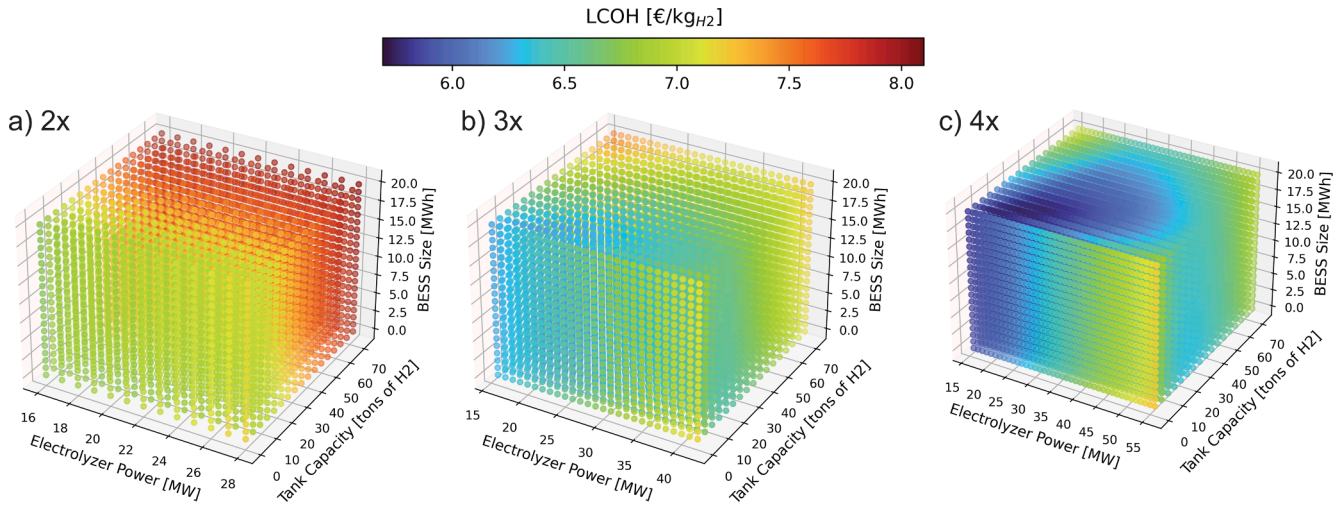

Fig. 12. LCOH indicators varying BESS capacity, tank capacity and electrolyzer power. Comparison among different wind farm size scales. All graphs use the same color scale.

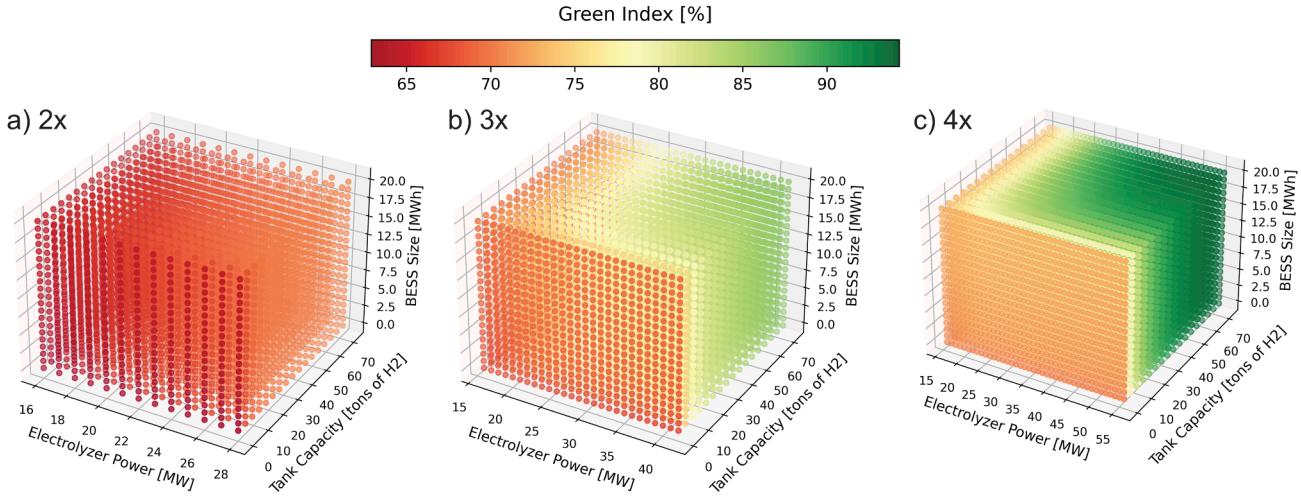

Fig. 13. GI indicators varying BESS capacity, tank capacity and electrolyzer power. Comparison among different wind farm scales. All graphs use the same color scale.

3.5.2. Price of electricity

Fig. 16 reports the trend of the Italian unified national price (PUN) during the past 3 years and a half: 2019 (a), 2020 (b), 2021 (c) and January to August 2022 (d). PUN history was obtained from the Italian electric market manager, "Gestore del Mercato Elettrico (GME)". Mean price recorded during the year is represented by the orange flat line, while the green flat line represents the price threshold of 20 €/MWh that is required to classify the hydrogen produced by means of that electricity as "green". Fig. 16 (a) shows that, during 2019, the price of electricity fluctuated around its mean value of 52 €/MWh, going below the "green threshold" only a few times. In 2020 (Fig. 16 (b)) the price dropped during the months of April and May (COVID-19 lockdown months) and raised again during the last months of the year. The situation changed radically in 2021 (Fig. 16 (c)) and in fist months of 2022 (Fig. 16 (d)), when the electricity price has seen a sharp rise starting from September 2021. Average electricity price rose considerably: 311 €/MWh in 2022, six times the average price of 2019. Due to this strong uncertainty behind the electricity expenditure that the system must face during its lifetime to support the constant hydrogen production, it is important to analyze how techno-economic metrics as the levelized cost of hydrogen and the green index would vary under different market conditions.

3.5.3. Market and components price variation

Fig. 17 shows the effect of a variation in the electricity purchase and selling price on the techno-economic outcome of the optimal configuration under different market circumstances. Lines in the graph show the trend of LCOH (dotted line) and GI (dashed line), as well as the tank size (continuous line) and electrolyzer power (dash-dotted line). For what concerns the electricity purchase price variation, a price range from 50 to 300 €/MWh was considered, to assess how the optimal solution varies if the scenario shifts from a normal situation (2019 with an average price of 52 €/MWh) to the current market situation (311 €/MWh on average and rising). Four possible selling prices were considered (60, 80, 100 and 120 €/MWh) to understand how the difference between the two price points may modify the optimal solution. Analyses consider a fixed electrolyzer price of 600 €/MW and a tank price of 400 €/kg. Fig. 17 shows that an increase in the grid electricity expenditure of the system produces a massive drop in the final LCOH: from around 2 €/kg when the when the market presents prices in the 2019 range of 50 €/MWh, it rises to 7 €/kg when the electricity reaches current values of 300 €/kg.

This clearly reflects the strong dependency of LCOH on the electricity price fluctuations, due to the required energy from the grid. However, the optimal storage size gradually increases as the electricity purchase

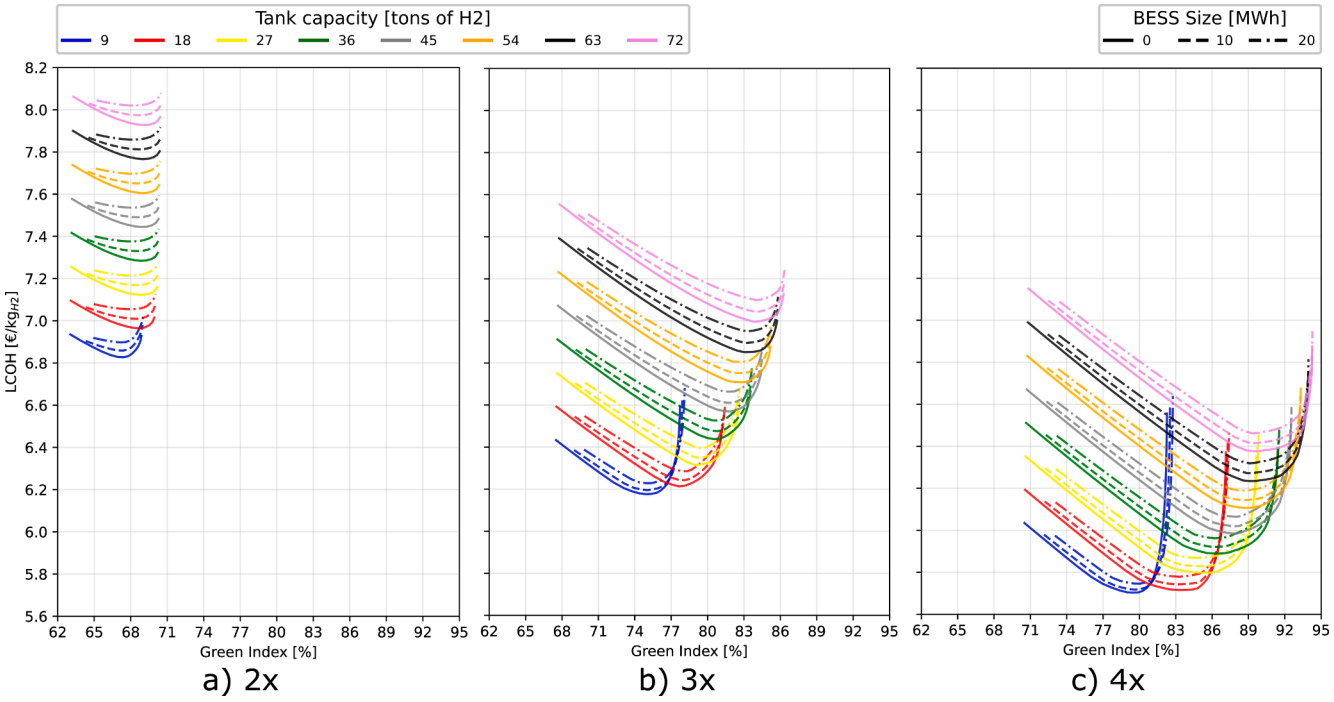

Fig. 14. LCOH value over GI varying BESS and tank size for three different farm scales (2x, 3x and 4x).

from the grid becomes more expensive, and this consequently rises the GI of the optimal solution: from less than 70% to more than 90%. The trade-off between the higher initial investment for a storage system and electricity savings shifts to bigger tank capacities. In the cheap electricity market scenario, the configuration without any storage means, i.e., the most gird-dependent one, is indeed the most convenient. The effect of the increase in the electricity selling price proves that the most important incentive for an investment on a storage system is given by the difference between the sale and purchase price: to parity of purchase price, a selling price of (120 €/MWh, red line) brings the GI of the optimal solution to significantly lower values with respect to solutions that considers a lower selling price (60 €/MWh, yellow line). If it is

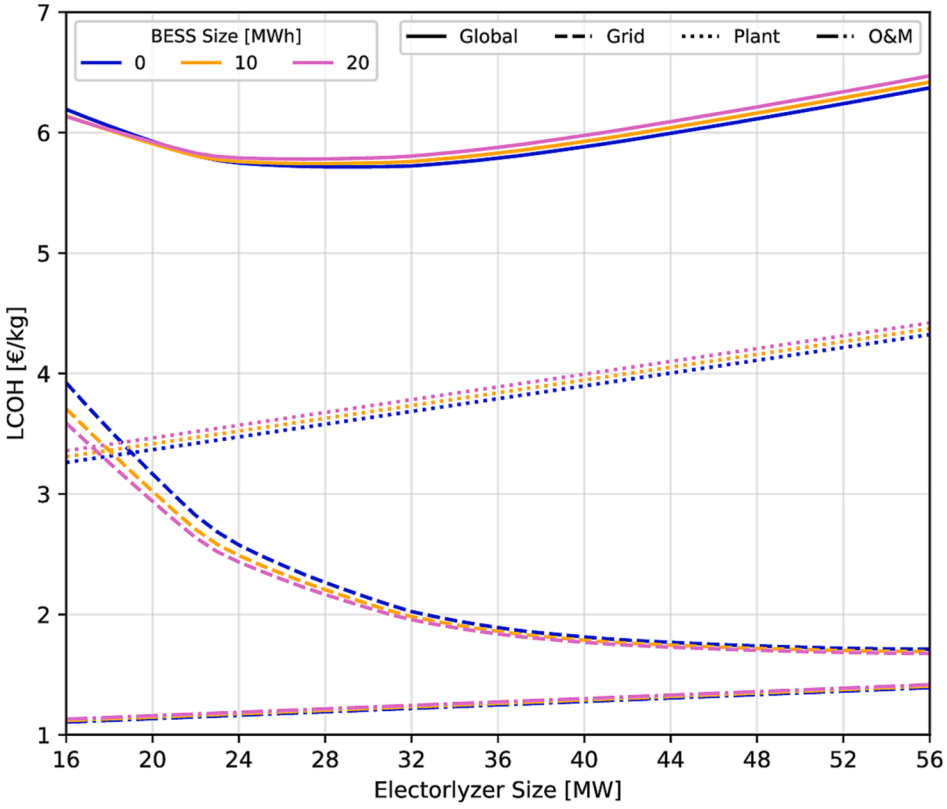

Fig. 15. LCOH contributors for a configuration provided with a tank capacity of or 9 tons of hydrogen and a BESS size of 0 MWh.

convenient to sell the excess energy, there is no advantage in investing in a storage system. Buying electricity from the grid during deficit hours would be more cost-effective.

Fig. 18 shows the effect of a reduction in the electrolyzer and tank price on the techno-economic outcome. Lines in two graphs show again the trend of the LCOH (dotted line) and GI (dashed line), as well as the tank size (continuous line) and electrolyzer power (dash-dotted line). An electrolyzer price drop from the actual value of 650 €/kW down to 200 €/kW was considered together with three tank prices: 400, 300 and 200 €/kg. A purchase price of electricity of 150 €/MWh and a selling price of 70 €/MWh were considered. This analysis shows that the effect of a reduction in the electrolyzer price also produces a considerable LCOH drop: a decrease on the investment price for the electrolyzer of almost 70% (650 to 200 €/kW) reduces the LCOH of around 1 €/kg. This time, it must be noticed that the price drop is followed by an increase in the GI. Cheaper components promote the installation of high-capacity storage systems that, in turn, enhance the self-sufficiency of the system. In the same way, a tank price drop reduces the LCOH and, since it pushes the installation of bigger tanks, makes the final product greener: to parity of electrolyzer cost, a tank price of 200 €/kg (light blue line) increases the GI of the optimal solution of around 3 percentage points with respect to a tank price of 400 €/kg.

Fig. 19 shows the effect of a BESS price reduction on the same quantities analyzed above. From a BESS starting price of 120 €/kWh, the analysis considers a price reduction down to 50 €/kWh, which corresponds approximately to a 60% reduction. For BESS prices higher than 100 €/kWh, results show that is not economically convenient to invest in this kind of storage. When the price falls below this threshold, the battery becomes a viable candidate. The optimal battery size increases steeply at price levels lower than 90 €/kWh: optimum of 1 MWh at 90 €/kWh, 5 MW at 80 €/kWh. In the latter point, the optimal tank capacity (continuous line) decreases from 13.5 to 9 tons of hydrogen, producing a drop in the GI (dashed line). This trend is determined by the discretized nature of the parametric analysis that may produce discontinuities on results. After this abrupt change, the optimal tank size remains constant, while a further drop in BESS price makes the optimal BESS size increase up to 20 MWh when the price is 50 €/kWh. Due to the small dimensions of this component with respect to the rest of the plant, this variation produces negligible changes on the LCOH (dotted line, 2c€/kg drop).

Table 4 summarizes the main results obtained by the sensitivity analyses on a) the electricity purchase and selling price variation, b) the electrolyzer and tank price variation and c) the battery price variation. Those results highlight the LCOH and the GI obtained at the maximum and minimum cost values considered for electricity and components. Additionally, it reports the optimal size of devices that best perform in each hypothetical market scenario.

3.5.4. potential impact of incentives

In a future scenario with rising electricity prices (accordingly to latest trends) and a drop in the cost of technologies, configurations that involve large storage systems able reach high levels of self-sufficiency seem promising. From the standpoint of a policy maker that aims to facilitate the decarbonization of hard-to-abate sectors as the steel manufacturing, those results help to understand where incentives could represent a catalyst of energy transition. Generally speaking, incentives targeted at lowering the expenditure in electricity purchase make the system less “clean” with respect to those on the capital cost of technologies. Fig. 20 reports the effect of the same amount of subsidy applied to electricity purchase price (Fig. 20 (a)) and electrolyzer price (Fig. 20 (b)). Both analyses consider, as a starting point, the configuration that brings to the lowest LCOH in a market condition in which the electricity purchase price is 150 €/MWh and the selling price is 70 €/MWh; the system comprises a 37 MW electrolyzer paired with a tank able to store 13.5 tons of hydrogen and no BESS.

This results in a LCOH of 5.7 €/kg and a GI of 82%. Fig. 20 (b) reports again the effect of a reduction in the electrolyzer price from 650 to 200 €/kW. To make a fair comparison between the impact of an incentive on components and an incentive on electricity purchase, the amount of money that is required to produce a certain drop in the electrolyzer price was first quantified. This was then converted in the equivalent achievable drop in electricity purchase. To reduce the component price of 450 €/kW when installing electrolyzer size of 37 MW, an incentive of 16.65 M€ is required. Considering the 20 years of lifetime for the analysis, this translates into an equivalent subsidy of 832.5 k€ per year. Since the initial optimal configuration requires 39.14 GWh per year, if this subsity is directed to reduce the electricity expenditure, it would result in a 21.27 €/MWh discount. Based on these assumptions, Fig. 20 (a) considers an electricity purchase price ranging from 128 to 150 €/MWh. The electrolyzer price reduction reduces the LCOH down to 4.93 €/kg and increases the GI up to 86%. On the other hand, the electricity purchase price reduction also decreases the LCOH, but to a lesser extent, down to 5.27 €/kg. In addition, this effect combines with a reduction of the GI of 6.5% due to the inconvenience of installing a large capacity tank and a high electrolyzer power. Not only the same subsidy produces a lower LCOH decrement when directed towards the electricity market, but also produces negative environmental impacts.

3.5.5. LCOH resilience to market fluctuations

Due to the uncertain trend of the grid electricity purchase price, it is worth assessing how the final LCOH varies when subjected to market fluctuations. For each configuration, this analysis focuses on the effect of the electricity purchase price variation on the resulting LCOH in configurations with different storages installed. Three different electrolyzer installed power rates are considered, namely 26, 36 and 46 MW.

Fig. 21 shows the relationship between the LCOH and the electricity purchase price variation (x axis). Lines of different colors (same for each of the three graphs) show the LOCH trend of configurations characterized by five different tank sizes: 0, 18, 36, 54 and 72 tons of hydrogen. The blue line represents the behavior of a configuration with no storage installed (16 MW electrolyzer, no tank). This can be considered as the reference for the most grid-dependent configuration, i.e., that providing the lowest LCOH when the grid electricity is cheap, although very sensitive to market fluctuations. Lines relative to a large installed tank results in a higher LCOH when the electricity purchase price is low (less than75 €/MWh) but starts becoming convenient when the price rises.

Fig. 22, similarly to Fig. 10, shows the LCOH variation according to the installed tank size, for increasing electricity purchase prices (represented in in different colors). A capacity range for the tank storage varying from 0 to 70 tons of hydrogen is considered. Fig. 22 (b) and Fig. 21 (c) show the LCOH minimums that the installation of a storage system produces when the electricity purchase price is sufficiently high and a consistent difference between the selling and purchase price is created. Fig. 22 (a) considers a minor electrolyzer power of 26 MW. The span between LCOH lines of different electricity purchase prices remains rather constant, even with increasing tank capacities. On the other hand, Fig. 22 (c) shows that, when large capacity tanks are coupled with higher electrolyzer power (46 MW), the distance between the LCOH lines can be reduced.

Fig. 21 and Fig. 22 also help in visualizing a key concept: a large installed tank, resulting in higher self-sufficiency of the system, makes the price of hydrogen less sensitive to the electric market fluctuation. If the electricity market sees a variation as the one that characterized the recent years (2020–2021), the average electricity price may vary from 50 to more than 300 €/MWh. For those two extremes, the LCOH generated by a grid-dependent configuration like the one adopting a16 MW of electrolyzer and no tank (blue line in Fig. 20) varies from less than 4 €/kg to almost 9 €/kg (a 125% increase). The LCOH derived from a configuration with a higher degree of self-sufficiency the one implementing a 46 MW of electrolyzer and 72 tons of hydrogen tank (pink line in graph (c)) sees a notably smaller variation, starting from a price of almost 6 €/kg and reaching a maximum price slightly higher than 7 €/kg, for a total variation around 1.5 €/kg. The resilience of self-

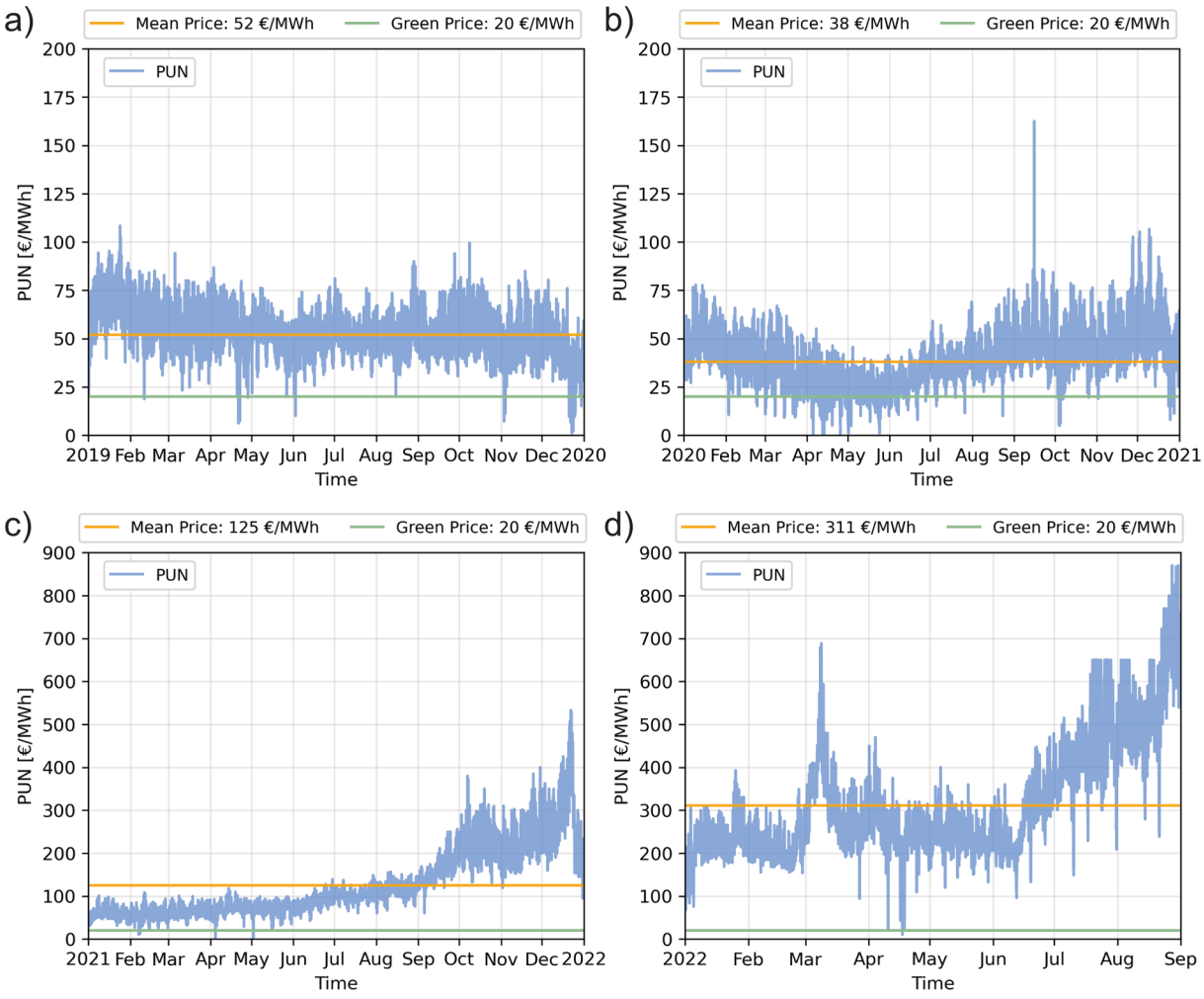

Fig. 16. Variation on Italian unified national price of electricity (PUN) for: a) 2019b) 2020c) 2021 d) January to August 2022. Average price recorded during the year is represented by the orange line. Green line represents the price threshold required to classify the hydrogen as "green".

sufficient systems to market variations in electricity price is key to understand the potential of storage systems in this kind of applications.

4. Emissions reduction

Based on the comprehensive analysis presented in the above paragraphs, this section aims to assess and quantify the effective decarbonization potential of the proposed solutions in the broader EU-27 context of steel production. A comparison is made with both the traditional BF-BOF route and with new generation H_2-SF-EAF plants that rely entirely on the electricity grid for energy supply.

On the basis of data available in the literature, an estimation of material flows, electricity consumption and related emissions has been carried out for the case study under consideration to align with the most widely established indicators. In this framework, it is important to consider that hydrogen-based steel production can be divided into three different sub-processes, namely the production of Hot-Briquetted Iron (HBI) in the shaft furnace, the iron-to-steel conversion in the EAF and the production and storage of the hydrogen required for the reduction process. All the calculations for material and energy flows, as well as for the emission factor, are ultimately referred to the production of one ton of liquid steel.

Vogl et al. [21] report that, for the process under consideration, 1504 kg of iron ore pellets are required per each ton of liquid steel produced, together with 51 kg of hydrogen as reducing agent for the same output. They also specify that, if the feedstock for the EAF is made of equal share of HBI and scrap, as it is in the assumptions of this study, the required volumes turn into 738 kg of iron ore, 536 kg of scrap material and 25 kg of hydrogen per ton of liquid steel. The definition of the material flows involved in the process is preliminary to the calculation of both specific consumption and emissions and to make it comparable to other case studies.

In terms of energy requirements, the H_2-SF-EAF route is reported to account for 4.25 MWh/tls by Bhaskar et al. [10], considering an electrolyzer efficiency of 53 kWh/kgH_2, for the techno-economic assessment of a grid connected plant located in Norway using 100% HBI. By adopting the method derived from the above-mentioned study, the corresponding figure for this work turns out to be 2.201 MWh/tls, considering a nominal efficiency of 56.2 kWh/kgH_2 for the electrolyzer technology adopted in this study. The great reduction in consumption is largely due to the use of a 50% share of scrap material. It is also worth noting that electrolysis in this case contributes about 65% of the total energy consumption for steel production.

Given these necessary assumptions, the specific emissions for the case study have been calculated accounting for the impact of wind-produced hydrogen, in order to accurately define the decarbonization potential of the proposed solutions. Total emissions can be classified into direct and indirect as made by Bhaskar et al. [10]. The only direct contribution is represented by emissions from EAF operations and accounts for 73 kgCO_2/tls, due to lime production, carbon oxidation and FeO reduction. Indirect emissions figures are also reported and re-adapted from [21] and [10], presenting values of 53 and 55.90

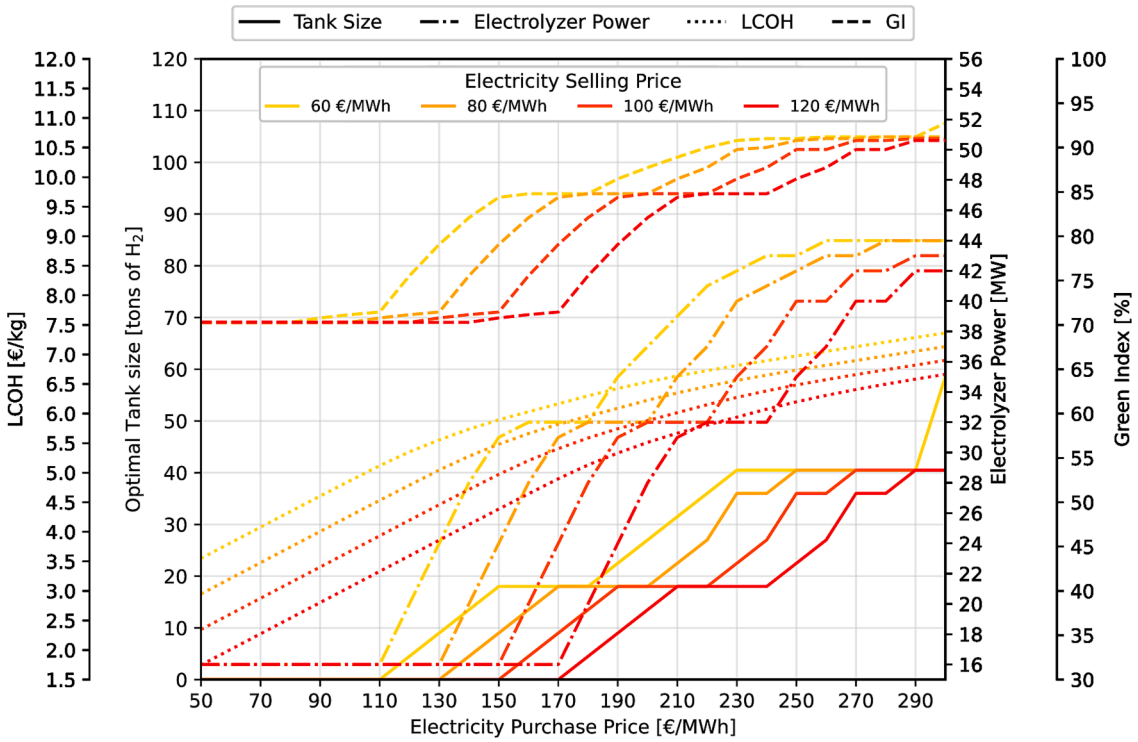

Fig. 17. Electricity purchase and selling price effect on the variation on optimal configuration parameters: LCOH (dotted line), GI (dashed line), tank size (continuous line) and electrolyzer size (dash-dotted line).

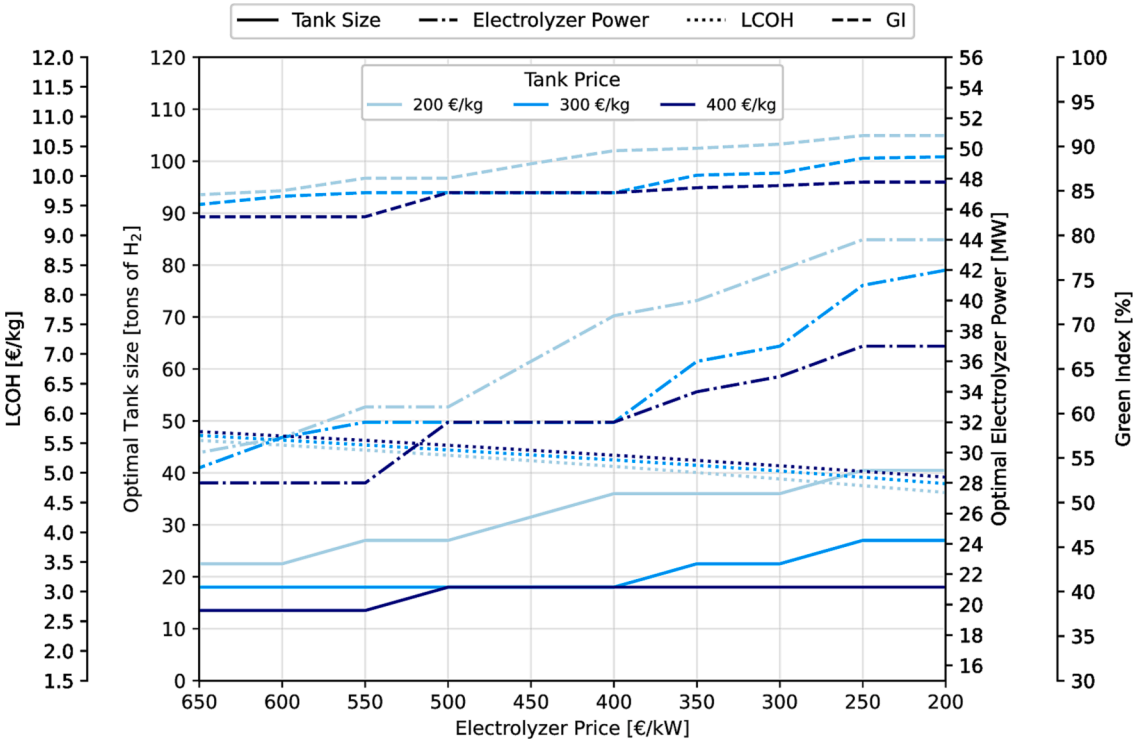

Fig. 18. Tank and electrolyzer price effect on the variation on optimal configuration parameters: LCOH (dotted line), GI (dashed line), tank size (continuous line) and electrolyzer size (dash-dotted line).

$kgCO_2$/tls respectively for carbon, lime and graphite electrodes consumption and for iron ore pellet. The parameter of main interest for the analysis is represented by the indirect emissions from electricity consumption, which is a function of both material flows and the emission intensity of the grid to which the plant is connected.

Fig. 23 shows the GI and the correspondent process emission reduction that can be achieved at different LCOH values. Starting from the price of the optimal configuration (5.7 €/kg), the graph shows how

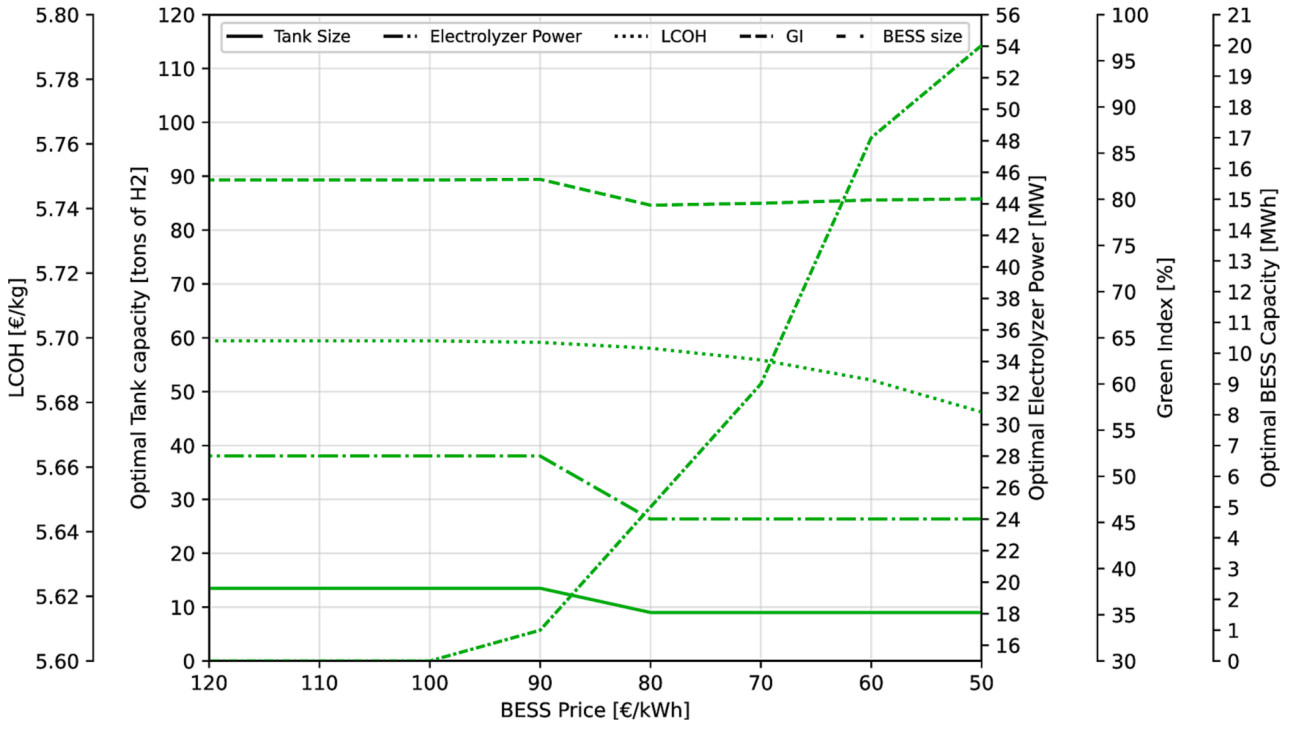

Fig. 19. BESS price effect on the variation on optimal configuration parameters as: LCOH (dotted line), GI (dashed line), tank size (continuous line) and electrolyzer size (dash-dotted line).

Table 4
Main outcomes of the sensitivity analysis on a) electricity purchase and selling price variation, b) electrolyzer and tank price variation and c) battery price variation.

El purchase price [€/MWh]	El selling price [€/MWh]	EC cost [€/kW]	Tank cost [€/kg]	BESS cost [€/kWh]	EC power [MW]	BESS size [MWh]	Tank size [tons of H2]	GI [%]	LCOH [€/kg]
a) Electricity price sensitivity analysis									
50*	120**	600	400	117	16	0	0	70.3	1.75
50*	60*	600	400	117	16	0	0	70.3	3.55
300**	120**	600	400	117	42	0	40	90.8	6.66
300**	60*	600	400	117	44	0	58	92.75	7.36
b) Electrolyzer and tank prices sensitivity analysis									
150	70	650**	400**	117	28	0	13	82	5.7
150	70	650**	200*	117	30	0	22	84.5	5.55
150	70	200*	400**	117	37	0	17	86	4.93
150	70	200*	200	117	44	0	40	91.2	4.67
c) Battery price sensitivity analysis									
150	70	650	400	120**	28	0	13	82	5.7
150	70	650	400	50*	24	20	9	80	5.67

* minimum and ** maximum price value considered in the sensitivity analyses.

the GI can increase if a higher cost is accepted, thanks to higher sizes of the storage systems. Direct emissions from reactions occurring in the electric arc furnace (EAF) are displayed in orange and are constant for all configurations. Global emissions from the entire process, in grey, vary according to the GI (green line) of the hydrogen fed to the plant. The optimal system size in economic terms does not match the most environmentally friendly solution and to reach higher green shares, the cost of the hydrogen must increase.

Three configurations, summarized in Table 5, have been selected as a reference and for comparison.

Configuration A leads to the lowest LCOH, thus the optimal solution in economic terms, and results in a LCOH of 5.7 €/kg. In this case the GI of the final product is around 82% - a remarkable result - which leads to a carbon intensity of the steel manufacturing process of 334 kg of CO_2 per ton of liquid steel. On the other hand, the most significant reduction can be achieved by configuration C, which brings to a GI of almost 96% but a considerably higher LCOH of 7.6 €/kg. In this case, the emission intensity can be lowered to 218 $kgCO_2$/tls. Between those two extremes there is a trade-off between price and emission savings: configuration B. In this case, for a hydrogen price of 6.5 €/kg, the GI can reach almost 94% and emissions can be reduced to 235 $kgCO_2$/tls.

For the sake of comparison, Fig. 24 presents the re-adaptation of data presented in the work of Bhaskar et al. [10] that compare the carbon intensity the H_2-DRI-EAF route in different countries, producing hydrogen from electrolysis that entirely relies on electricity from the national grid (yellow hydrogen). The graph also reports the country-related emissions of the natural gas driven manufacturing process NG-DRI- EAF (red dots) and the emission band of the traditional manufacturing pathway based on blast furnace (grey bands).

The three case studies illustrated above are included in the graph

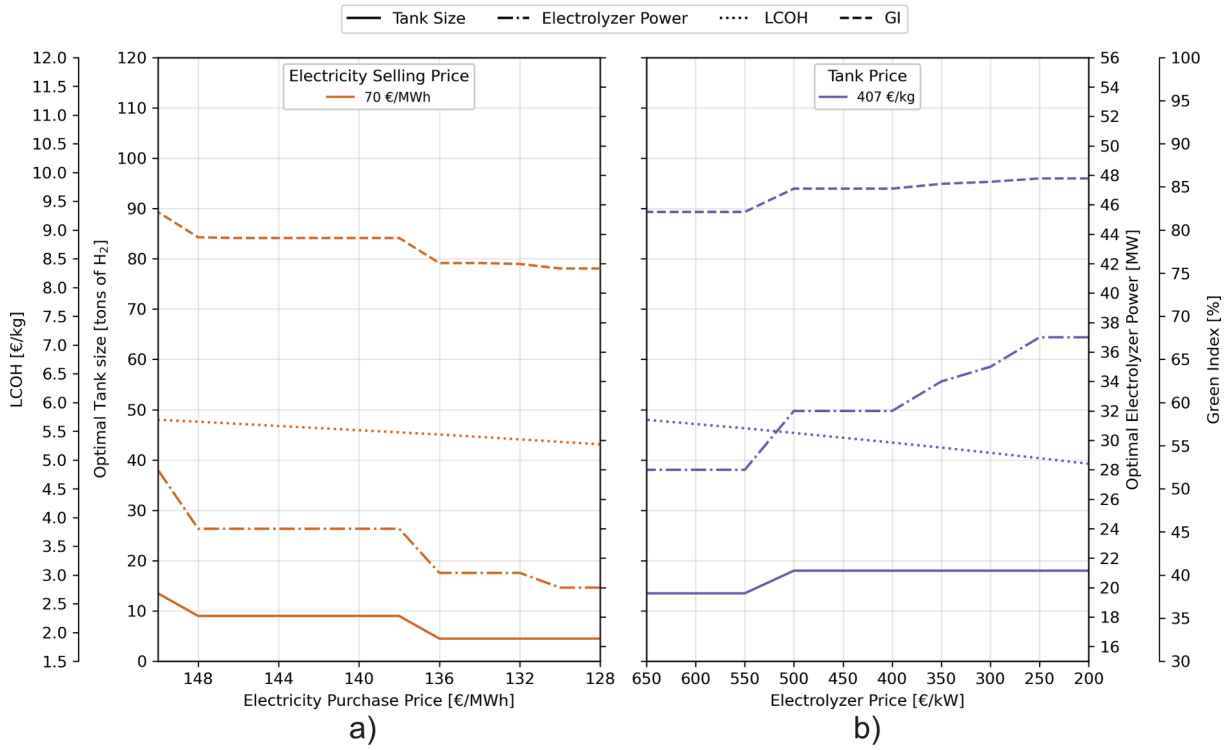

Fig. 20. Incentive comparison of the same magnitude on a) electricity purchase price and b) electrolyzer price.

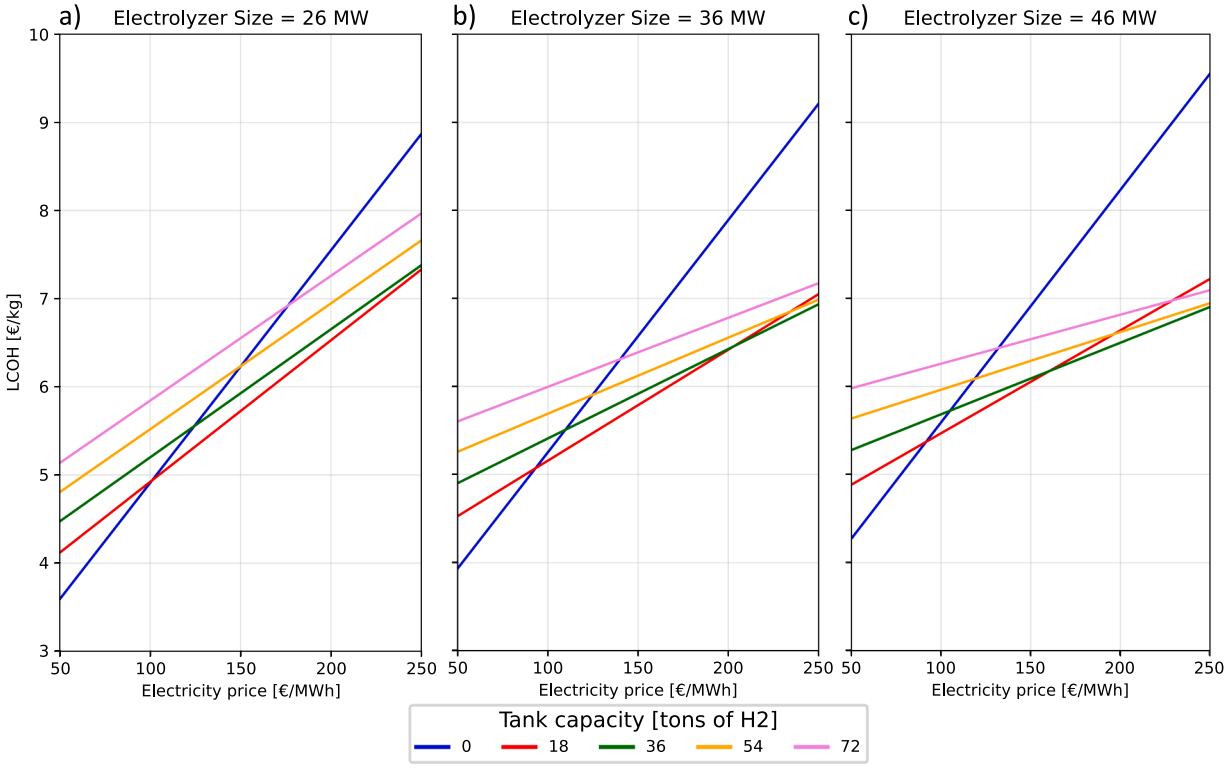

Fig. 21. LCOH trends by varying electricity price and tank size for three different electrolyzer sizes: 26 (a), 36 (b) and 46 MW (c).

next to the bar representing the Italian scenario. In Italy, due to the high reliance on fossil fuels for electricity production, a steel manufacturing process that fully relies on yellow hydrogen can reach emissions of almost 1 tCO_2/tls, even higher than NG-EAF (844 $kgCO_2$/tls). The three proposed configurations show considerably lower specific emissions. The carbon intensity of a process that utilizes hydrogen produced by configuration A would be comparable to what can be achieved in France or Finland, i.e., countries in which the electricity generation highly relies on low carbon sources. Using configurations B and C the result starts to approach even less carbon intensive countries as Norway. This

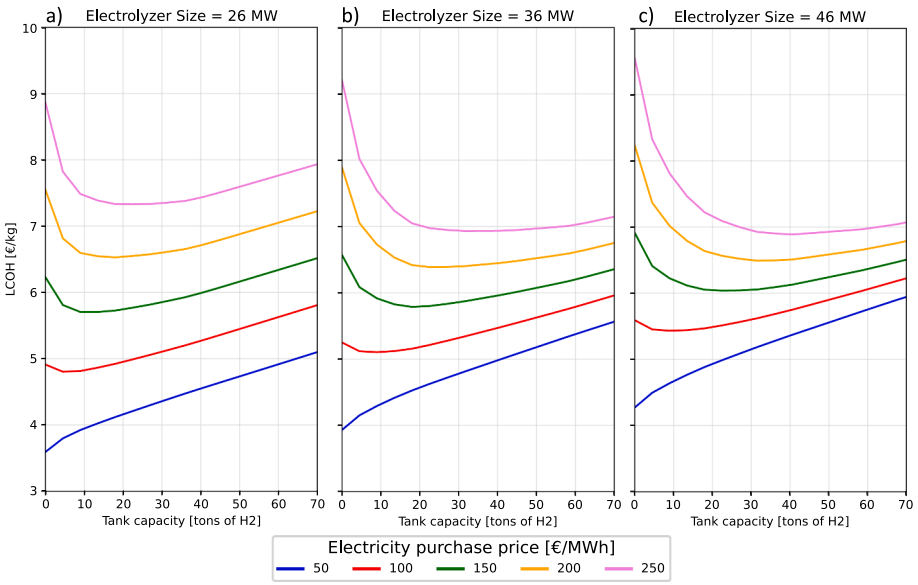

Fig. 22. LCOH varying electricity price and tank size for three different electrolyzer sizes: 26 (a), 36 (b) and 46 MW (c).

comparison shows that, in a country in which electricity generation is still relying on non-renewable fuel sources, hydrogen production systems that directly exploits the energy produced by renewable power stations are the only way to decarbonize hard-to-abate processes as the steel manufacturing.

5. Conclusions

The study provides a techno-economic analysis on the potential production of a constant flow rate of green hydrogen for an industrial user fed by a dedicated wind farm. A steel mill was selected as the hypothetical final user of the produced hydrogen. The industrial demand was modelled on a H_2-DRI-EAF steel making process, considering the new small-scale plant concept that processes half scrap and half raw materials. The decarbonization of the steel production sector is part of the path towards a cleaner manufacturing industry. In that context, green hydrogen can play a key role in achieving the greenhouse emissions reduction goals of our society. Real data from an existing wind farm were used to estimate the producibility of such systems. The rise of the intermittent renewable energy generation opens new possibilities for producing hydrogen in a sustainable way, but also brings new challenges. Real data from an existing wind farm were used to estimate the producibility of such systems. Due to the intermittent nature of wind power production, two storage means were also considered and compared to match wind fluctuations with the constant request of the steel mill, namely batteries and hydrogen tanks. In addition, alkaline

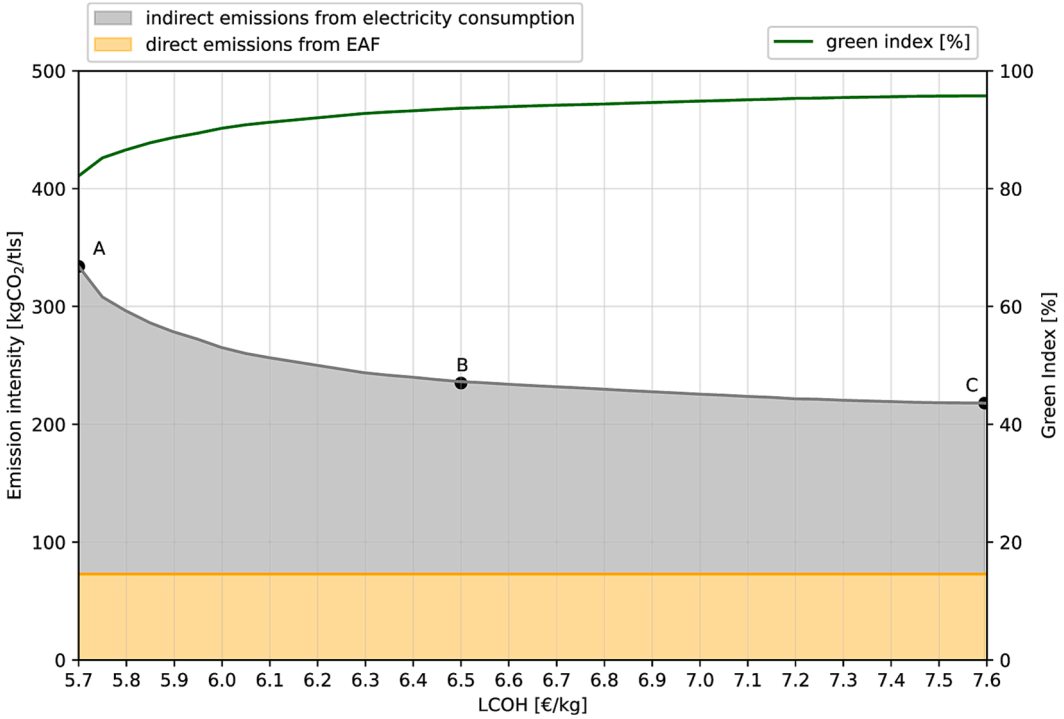

Fig. 23. Emission intensity and GI varying the LCOH of the system.

Table 5
Configurations for comparison.

Conf.	Electrolyzer power [MW]	Battery Capacity [MWh]	Tank Capacity [tons of H_2]	GI [%]	Emission intensity [$kgCO_2$/tls]	LCOH [€/kg]
A	28	1	13.5	82	334	5.7
B	48	4	68	94	235	6.5
C	56	17	117	96	218	7.6

electrolyzers and lithium-ion batteries models that account for aging and degradation effects were employed to simulate a realistic behavior under the fluctuating operation regime that they will face.

Several system configurations were considered, and their techno-economic outcome was evaluated by means of two parameters, namely the green index (GI), which considers the self-consumption of the system and the share of renewables in the national electric grid, and the Levelized Cost of Hydrogen (LCOH).

Results show that it is not possible to reach a 100% green hydrogen flow through the whole year, unless the wind farm is significantly oversized, which makes anyhow the investment not convenient. It must be stressed out that, due to the intermittent nature of wind power production, the national grid support still plays a key role in meeting the constant hydrogen demand. Nevertheless, storage means are key to increase the self-consumption of the system, the resulting green index, and the global emission reduction potential of the process. This latter point was thoroughly addressed by accounting for different configurations of the system. In particular, it is shown that it is not convenient to invest in a large capacity battery to store electricity upstream the electrolyzer. The best option to reach a high share of green hydrogen, while guaranteeing the constant flow rate needed to meet steel mill demand, is to enlarge the downstream storage capacity of the system, allowing the electrolyzer stack to follow the power fluctuations of the wind farm.

Furthermore, four different upscaling of the original wind farm were analyzed to adapt the power production potential to the constant request of the electrolyzers (16 MW). Electrolyzers power levels from 16 to 56 MW were considered, coupled with battery capacities ranging from 0 to 20 MWh and tanks able to store from 0 to 117 tons of hydrogen. Global results show that the configuration enabling to reach the lowest levelized cost of hydrogen consists in a large-scale wind farm (4 times the original one), coupled with 28 MW electrolyzers, a 1 MWh battery and tanks able to contain 13.5 tons of hydrogen; with this configuration, the resulting LCOH is 5.7 €/kg, with a GI of 82%. If the electrolyzer cost is decreased to 200 €/kW, due to the future market development or thanks to incentives, the optimal configuration could possibly reach a LCOH of 4.93 €/kg, still considerably higher than current grey hydrogen price (1–2 €/kg). Inevitably, a hydrogen production system that must provide a constant flow rate of gas is still dependent on grid electricity, whose high cost still hinders the potential cost reduction.

The sensitivity analysis conducted over the price of electricity and the capital investment of components shows that it is key to reduce the individual cost technologies (electrolyzers, batteries and tanks) to both reduce the LCOH and increase the green index. Among the various components, the electrolyzer price has shown the most relevant influence on the LCOH trend and is the most likely to decline in the near

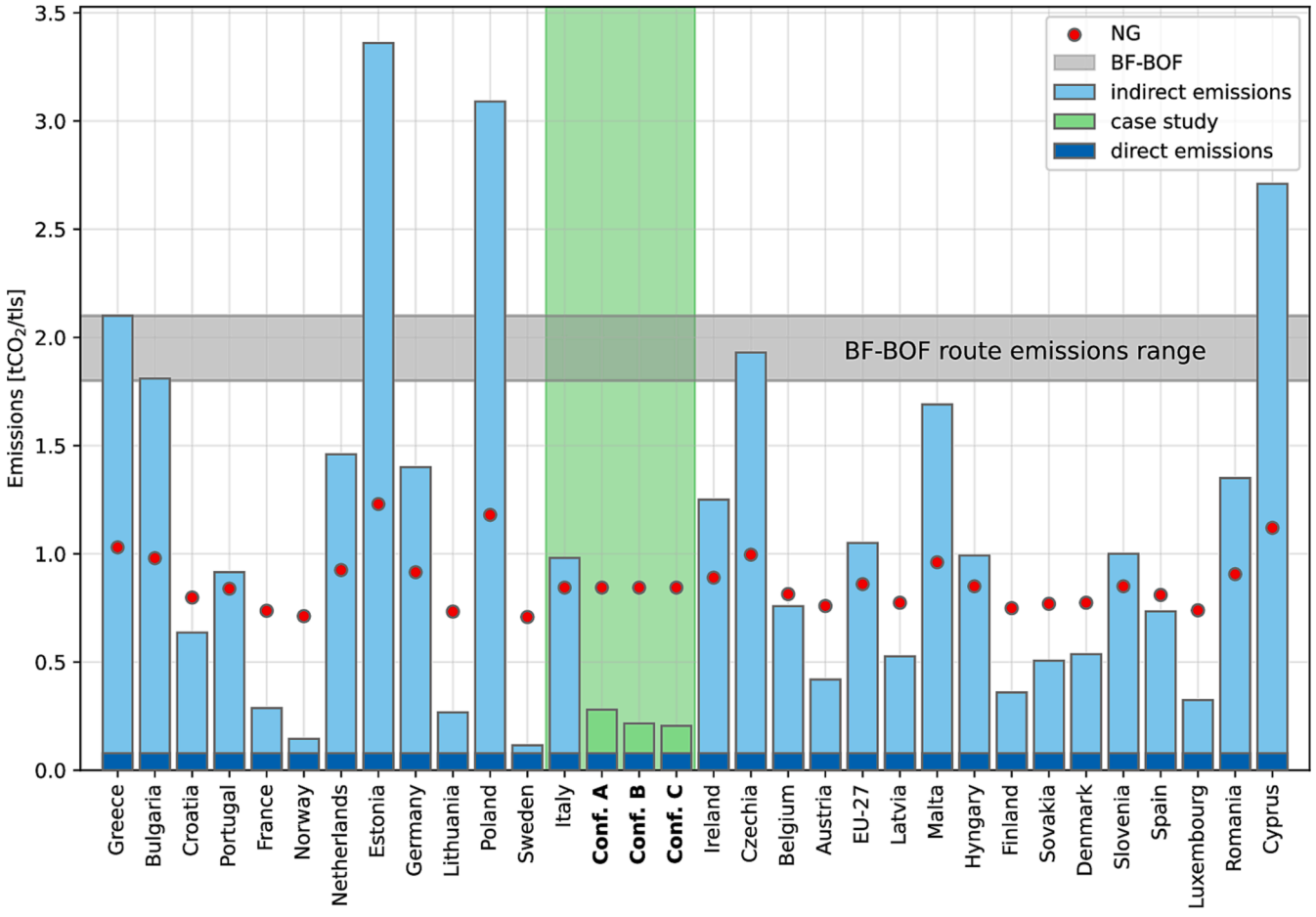

Fig. 24. Emission intensity for steel manufacturing in EU-27 countries, re. adapted from [10]

future. A price drop of 70% in electrolysis technologies would produce a 1 €/kg reduction on the final LCOH. Regarding storage means, a 50% cost reduction in tanks would have a smaller effect on the final hydrogen price but could increase the green index of the optimal solution up to 7%. On the other hand, a sensitivity analysis has shown that a large-scale battery storage would be economically unsustainable to reach high levels of self-sufficiency with respect to tanks. Due to the relatively small size range considered in the size optimization, the contribution of this component to the final LCOH is negligible (i.e., 2c€/kg for a 60% price drop of the component). A decline in electricity purchase prices would be crucial to reduce the cost of hydrogen, but it is very difficult to state how the electricity market might evolve even in the nearest future. These results are of particular interest for policy makers aiming to push forward the penetration of green hydrogen in industrial processes, since it is apparent that incentives should be focused on the reduction of components prices rather than on electricity purchase prices. Configurations that involve high-capacity storage means have been also proved to be more resilient to the electricity market fluctuations. One conceivable way to reduce both the cost of producing hydrogen and its carbon footprint is to decarbonize the electricity grid itself.

Results show that the emission reduction potential of hydrogen streams characterized by a high green index is remarkable. The emission intensity of a H_2-DRI-EAF steelmaking process located in Italy that takes as input the hydrogen mix of the most cost-effective configuration stands at around 334 $kgCO_2$/tls, a reduction of almost 84% if compared to the traditional BF-BOF process. This quantity can be further reduced if higher costs of hydrogen are accepted: the emission intensity of configurations presenting green indexes of 94% corresponds to 235 $kgCO_2$/tls, but a LOCH of 6.5 €/kg must be taken into account. As for the Italian energy mix, the emission intensity of the same process powered by grid electricity would be more than four times higher (1000 $kgCO_2$/tls). In countries where the electrical grid is still heavily dependent on fossil fuels, plants similar to the one analyzed in this work could enable a carbon reduction of the steel making process similar to what can be achieved in countries whose electrical grid is characterized by a really small carbon footprint.

Finally, upon examination of the potential emission reduction of the steelmaking process, it is shown that, in a country in which electricity generation is still relying on non-renewable fuel sources, hydrogen production systems that directly exploits the energy produced by renewable power stations are the only way to decarbonize hard-to-abate processes as the steel manufacturing.

CRediT authorship contribution statement

Francesco Superchi: Methodology, Software, Validation, Formal analysis, Investigation, Data curation, Writing – original draft, Visualization. **Alessandro Mati:** Software, Validation, Formal analysis, Investigation, Data curation, Writing – original draft. **Carlo Carcasci:** Resources, Supervision, Project administration, Funding acquisition. **Alessandro Bianchini:** Conceptualization, Methodology, Investigation, Resources, Data curation, Writing – review & editing, Supervision, Project administration, Funding acquisition.

Declaration of Competing Interest

The authors declare that they have no known competing financial interests or personal relationships that could have appeared to influence the work reported in this paper.

Data availability

Data will be made available on request.

Acknowledgements

This research did not receive any specific grant from funding agencies in the public, commercial, or not-for-profit sectors.

The authors would like to sincerely thank Eng. Mattia Pasqui for the intellectual assistance and support received during the conceptualization of this work.

References

[1] Energy Transitions Commission, "Mission Possible: Reaching Net-Zero Carbon Emissions - ETC," 2018. https://www.energy-transitions.org/publications/mission-possible/ (accessed Dec. 02, 2022).
[2] Schleussner C-F, et al. Science and policy characteristics of the Paris Agreement temperature goal. Nat Clim Chang 2016;6(9):827–35. https://doi.org/10.1038/nclimate3096.
[3] Iea. Iron and Steel Technology Roadmap. Paris 2020;2020. https://doi.org/10.1787/3dcc2a1b-en.
[4] "World Steel in Figures 2022 - worldsteel.org." https://worldsteel.org/steel-topics/statistics/world-steel-in-figures-2022/ (accessed Oct. 17, 2022).
[5] IEA, "IEA (2021)," Paris, 2021. doi: 10.1787/90c8c125-en.
[6] M. D. Fenton and C. A. Tuck, "Iron and Steel. 2016 Minerals Yearbook," *US Geol. Surv.*, 2019.
[7] Zhao J, Zuo H, Wang Y, Wang J, Xue Q. Review of green and low-carbon ironmaking technology. Ironmak Steelmak 2020;47(3):296–306. https://doi.org/10.1080/03019233.2019.1639029.
[8] "Iron and Steel – Analysis - IEA." https://www.iea.org/reports/iron-and-steel (accessed Mar. 29, 2023).
[9] Lee H, Lee J, Koo Y. Economic impacts of carbon capture and storage on the steel industry–A hybrid energy system model incorporating technological change. Appl Energy Jul. 2022;317:119208. https://doi.org/10.1016/J.APENERGY.2022.119208.
[10] Bhaskar A, Abhishek R, Assadi M, Somehesaraei HN. Decarbonizing primary steel production: Techno-economic assessment of a hydrogen based green steel production plant in Norway. J Clean Prod 2022;vol. 350, no. March:131339. https://doi.org/10.1016/j.jclepro.2022.131339.
[11] Nwachukwu CM, Olofsson E, Lundmark R, Wetterlund E. Evaluating fuel switching options in the Swedish iron and steel industry under increased competition for forest biomass. Appl Energy Oct. 2022;324:119878. https://doi.org/10.1016/J.APENERGY.2022.119878.
[12] H. Suopajärvi *et al.*, "Use of biomass in integrated steelmaking – Status quo, future needs and comparison to other low-CO2 steel production technologies," *Appl. Energy*, vol. 213, no. November 2017, pp. 384–407, 2018, doi: 10.1016/j.apenergy.2018.01.060.
[13] Jahanshahi S, et al. Development of Low-Emission Integrated Steelmaking Process. J Sustain Metall 2015;1(1):94–114. https://doi.org/10.1007/s40831-015-0008-6.
[14] Toktarova A, Walter V, Göransson L, Johnsson F. Interaction between electrified steel production and the north European electricity system. Appl Energy 2022;310 (January). https://doi.org/10.1016/j.apenergy.2022.118584.
[15] "PROCESS INTEGRATION IN THE IRON AND STEEL INDUSTRY: IEA IETS ANNEX XIV TECHNICAL REPORT," Accessed: Mar. 29, 2023. [Online]. Available: http://www.iea-industry.org.
[16] World Steel Association, "STEEL ' S CONTRIBUTION TO A LOW CARBON FUTURE AND CLIMATE RESILIENT SOCIETIES worldsteel position paper," *World Steel Assoc.*, pp. 1–6, 2015, [Online]. Available: http://www.worldsteel.org/dms/internetDocumentList/bookshop/Steel-s-Contribution-to-a-Low-Carbon-Future-/document/Steel's Contribution to a Low Carbon Future .pdf.
[17] Nwachukwu CM, Toffolo A, Wetterlund E. Biomass-based gas use in Swedish iron and steel industry – Supply chain and process integration considerations. Renew Energy Feb. 2020;146:2797–811. https://doi.org/10.1016/J.RENENE.2019.08.100.
[18] S. Tian, J. Jiang, Z. Zhang, and V. Manovic, "Inherent potential of steelmaking to contribute to decarbonisation targets via industrial carbon capture and storage," doi: 10.1038/s41467-018-06886-8.
[19] "Impact of Hydrogen DRI on EAF Steelmaking - Midrex Technologies, Inc." https://www.midrex.com/tech-article/impact-of-hydrogen-dri-on-eaf-steelmaking/ (accessed Mar. 29, 2023).
[20] Fan Z, Friedmann SJ. Low-carbon production of iron and steel: Technology options, economic assessment, and policy. Joule Apr. 2021;5(4):829–62. https://doi.org/10.1016/J.JOULE.2021.02.018.
[21] Vogl V, Åhman M, Nilsson LJ. Assessment of hydrogen direct reduction for fossil-free steelmaking. J Clean Prod 2018;203:736–45. https://doi.org/10.1016/j.jclepro.2018.08.279.
[22] Fischedick M, Marzinkowski J, Winzer P, Weigel M. Techno-economic evaluation of innovative steel production technologies. J Clean Prod 2014;84(1):563–80. https://doi.org/10.1016/J.JCLEPRO.2014.05.063.
[23] M. Pei, M. Petäjäniemi, A. Regnell, and O. Wijk, "metals Toward a Fossil Free Future with HYBRIT: Development of Iron and Steelmaking Technology in Sweden and Finland," doi: 10.3390/met10070972.
[24] "HYBRIT pilot plant produces first sponge iron using fossil-free hydrogen gas | S&P Global Commodity Insights." https://www.spglobal.com/commodityinsights/en/

market-insights/latest-news/electric-power/062121-hybrit-pilot-plant-produces-first-sponge-iron-using-fossil-free-hydrogen-gas (accessed Oct. 18, 2022).
[25] "Hydrogen-based steelmaking to begin in Hamburg | ArcelorMittal." https://corporate.arcelormittal.com/media/case-studies/hydrogen-based-steelmaking-to-begin-in-hamburg (accessed Oct. 18, 2022).
[26] V. Vogl *et al.*, "Green Steel Tracker." Stockholm, 2021, [Online]. Available: www.industrytransition.org/green-steel-tracker.
[27] Bhaskar A, Assadi M, Somehsaraei HN. Decarbonization of the iron and steel industry with direct reduction of iron ore with green hydrogen. Energies 2020;13(3):1–23. https://doi.org/10.3390/en13030758.
[28] Davis SJ, et al. Net-zero emissions energy systems. Science (80-.) Jun. 2018;360(6396). https://doi.org/10.1126/SCIENCE.AAS9793.
[29] Dinh VN, Leahy P, McKeogh E, Murphy J, Cummins V. Development of a viability assessment model for hydrogen production from dedicated offshore wind farms. Int J Hydrogen Energy Jul. 2021;46(48):24620–31. https://doi.org/10.1016/J.IJHYDENE.2020.04.232.
[30] Lucas TR, Ferreira AF, Santos Pereira RB, Alves M. Hydrogen production from the WindFloat Atlantic offshore wind farm: A techno-economic analysis. Appl Energy Mar. 2022;310. https://doi.org/10.1016/J.APENERGY.2021.118481.
[31] Franco BA, Baptista P, Neto RC, Ganilha S. Assessment of offloading pathways for wind-powered offshore hydrogen production: Energy and economic analysis. Appl Energy Mar. 2021;286:116553. https://doi.org/10.1016/J.APENERGY.2021.116553.
[32] McDonagh S, Ahmed S, Desmond C, Murphy JD. Hydrogen from offshore wind: Investor perspective on the profitability of a hybrid system including for curtailment. Appl Energy 2020;vol. 265, no. February:114732. https://doi.org/10.1016/j.apenergy.2020.114732.
[33] Olateju B, Kumar A, Secanell M. A techno-economic assessment of large scale wind-hydrogen production with energy storage in Western Canada. Int J Hydrogen Energy 2016;41(21):8755–76. https://doi.org/10.1016/j.ijhydene.2016.03.177.
[34] Weimann L, Gabrielli P, Boldrini A, Kramer GJ, Gazzani M. Optimal hydrogen production in a wind-dominated zero-emission energy system. Adv Appl Energy Aug. 2021;3. https://doi.org/10.1016/J.ADAPEN.2021.100032.
[35] Glenk G, Reichelstein S. Economics of converting renewable power to hydrogen. Nat Energy 2019;4(3):216–22. https://doi.org/10.1038/s41560-019-0326-1.
[36] Saba SM, Müller M, Robinius M, Stolten D. The investment costs of electrolysis – A comparison of cost studies from the past 30 years. Int J Hydrogen Energy Jan. 2018;43(3):1209–23. https://doi.org/10.1016/J.IJHYDENE.2017.11.115.
[37] Shiva Kumar S, Himabindu V. Hydrogen production by PEM water electrolysis – A review. Mater Sci Energy Technol Dec. 2019;2(3):442–54. https://doi.org/10.1016/J.MSET.2019.03.002.
[38] "Nel ASA: Receives 4.5 MW electrolyzer purchase order for fossil free steel production | Nel Hydrogen." https://nelhydrogen.com/press-release/nel-asa-receives-4-5-mw-electrolyzer-purchase-order-for-fossil-free-steel-production/ (accessed Oct. 26, 2022).
[39] Schmidt O, Gambhir A, Staffell I, Hawkes A, Nelson J, Few S. Future cost and performance of water electrolysis: An expert elicitation study. Int J Hydrogen Energy Dec. 2017;42(52):30470–92. https://doi.org/10.1016/J.IJHYDENE.2017.10.045.
[40] Marini S, et al. Advanced alkaline water electrolysis. Electrochim Acta Nov. 2012;82:384–91. https://doi.org/10.1016/J.ELECTACTA.2012.05.011.
[41] Ursúa A, Barrios EL, Pascual J, San Martín I, Sanchis P. Integration of commercial alkaline water electrolysers with renewable energies: Limitations and improvements. Int J Hydrogen Energy Aug. 2016;41(30):12852–61. https://doi.org/10.1016/J.IJHYDENE.2016.06.071.
[42] Liponi A, Baccioli A, Ferrari L, Desideri U. Techno-economic analysis of hydrogen production from PV plants. E3S Web Conf 2022;334:01001. https://doi.org/10.1051/e3sconf/202233401001.
[43] Usman MR. Hydrogen storage methods: Review and current status. Renew Sustain Energy Rev Oct. 2022;167:112743. https://doi.org/10.1016/J.RSER.2022.112743.
[44] Abe JO, Popoola API, Ajenifuja E, Popoola OM. Hydrogen energy, economy and storage: Review and recommendation. Int J Hydrogen Energy Jun. 2019;44(29):15072–86. https://doi.org/10.1016/J.IJHYDENE.2019.04.068.
[45] Zhang F, Zhao P, Niu M, Maddy J. The survey of key technologies in hydrogen energy storage. Int J Hydrogen Energy Sep. 2016;41(33):14535–52. https://doi.org/10.1016/J.IJHYDENE.2016.05.293.
[46] Meier K. Hydrogen production with sea water electrolysis using Norwegian offshore wind energy potentials: Techno-economic assessment for an offshore-based hydrogen production approach with state-of-the-art technology. Int J Energy Environ Eng Jul. 2014;5(2–3):1–12. https://doi.org/10.1007/S40095-014-0104-6/TABLES/6.
[47] Correa G, Volpe F, Marocco P, Muñoz P, Falagüerra T, Santarelli M. Evaluation of levelized cost of hydrogen produced by wind electrolysis: Argentine and Italian production scenarios. J Energy Storage Aug. 2022;52. https://doi.org/10.1016/J.EST.2022.105014.
[48] Nascimento da Silva G, Rochedo PRR, Szklo A. Renewable hydrogen production to deal with wind power surpluses and mitigate carbon dioxide emissions from oil refineries. Appl Energy Apr. 2022;311. https://doi.org/10.1016/J.APENERGY.2022.118631.
[49] Eurofer, *European steel in figures 2022*. 2022.
[50] "World Steel in Figures 2022 - worldsteel.org." https://worldsteel.org/steel-topics/statistics/world-steel-in-figures-2022/ (accessed Mar. 30, 2023).
[51] "Danieli." https://www.danieli.com/it/about-us/storia/integrated-minimills_18_14.htm (accessed Nov. 08, 2022).
[52] "MINIMILLS and INTEGRATED PLANTS | Metech STG." http://www.stggroup.it/en/plants/minimills (accessed Nov. 08, 2022).
[53] "Hydrogen steel plant: voestalpine X Mitsubishi Heavy Industries | EU-Japan." https://www.eu-japan.eu/publications/hydrogen-steel-plant-voestalpine-x-mitsubishi-heavy-industries (accessed Nov. 08, 2022).
[54] "Hydrogen-based steelmaking to begin in Hamburg | ArcelorMittal." https://corporate.arcelormittal.com/media/case-studies/hydrogen-based-steelmaking-to-begin-in-hamburg (accessed Nov. 08, 2022).
[55] Ajanovic A, Sayer M, Haas R. The economics and the environmental benignity of different colors of hydrogen. Int J Hydrogen Energy 2022;no. xxxx. https://doi.org/10.1016/j.ijhydene.2022.02.094.
[56] Superchi F, Papi F, Mannelli A, Balduzzi F, Ferro FM, Bianchini A. Development of a reliable simulation framework for techno-economic analyses on green hydrogen production from wind farms using alkaline electrolyzers. Renew Energy May 2023;207:731–42. https://doi.org/10.1016/J.RENENE.2023.03.077.
[57] A. Mannelli, F. Papi, G. Pechlivanoglou, G. Ferrara, and A. Bianchini, "Discrete Wavelet Transform for the Real-Time Smoothing of Wind Turbine Power Using Li-Ion Batteries," *Energies 2021, Vol. 14, Page 2184*, vol. 14, no. 8, p. 2184, Apr. 2021, doi: 10.3390/EN14082184.
[58] Divya KC, Østergaard J. Battery energy storage technology for power systems-An overview. Electr Power Syst Res Apr. 2009;79(4):511–20. https://doi.org/10.1016/J.EPSR.2008.09.017.
[59] Mah AXY, et al. Optimization of a standalone photovoltaic-based microgrid with electrical and hydrogen loads. Energy Nov. 2021;235. https://doi.org/10.1016/J.ENERGY.2021.121218.
[60] Nicita A, Maggio G, Andaloro APF, Squadrito G. Green hydrogen as feedstock: Financial analysis of a photovoltaic-powered electrolysis plant. Int J Hydrogen Energy Apr. 2020;45(20):11395–408. https://doi.org/10.1016/j.ijhydene.2020.02.062.
[61] Jang D, Kim K, Kim KH, Kang S. Techno-economic analysis and Monte Carlo simulation for green hydrogen production using offshore wind power plant. Energy Convers Manag Jul. 2022;263. https://doi.org/10.1016/J.ENCONMAN.2022.115695.
[62] Superchi F, Mati A, Pasqui M, Carcasci C, Bianchini A. Techno-economic study on green hydrogen production and use in hard-to-abate industrial sectors. J Phys Conf Ser 2022.
[63] Lubello P, Pasqui M, Mati A, Carcasci C. "Assessment of hydrogen based long term electrical energy storage in residential energy systems", *Smart. Energy* 2022;vol. 8, no. August:100088. https://doi.org/10.1016/j.segy.2022.100088.
[64] Singlitico A, Østergaard J, Chatzivasileiadis S. Onshore, offshore or in-turbine electrolysis? Techno-economic overview of alternative integration designs for green hydrogen production into Offshore Wind Power Hubs. Renew Sustain Energy Transit Aug. 2021;1:100005. https://doi.org/10.1016/J.RSET.2021.100005.
[65] Kazi MK, Eljack F, El-Halwagi MM, Haouari M. Green hydrogen for industrial sector decarbonization: Costs and impacts on hydrogen economy in qatar. Comput Chem Eng Feb. 2021;145. https://doi.org/10.1016/J.COMPCHEMENG.2020.107144.
[66] Duffy A, et al. Land-based wind energy cost trends in Germany, Denmark, Ireland, Norway, Sweden and the United States. Appl Energy Nov. 2020;277. https://doi.org/10.1016/J.APENERGY.2020.114777.
[67] Wang R, Lam CM, Hsu SC, Chen JH. Life cycle assessment and energy payback time of a standalone hybrid renewable energy commercial microgrid: A case study of Town Island in Hong Kong. Appl Energy Sep. 2019;250:760–75. https://doi.org/10.1016/J.APENERGY.2019.04.183.
[68] S. Furfari and A. Clerici, "Green hydrogen: the crucial performance of electrolysers fed by variable and intermittent renewable electricity," *Eur. Phys. J. Plus*, vol. 136, no. 5, May 2021, doi: 10.1140/EPJP/S13360-021-01445-5.
[69] D. Pivetta, C. Dall'armi, and R. Taccani, "Multi-Objective Optimization of a Hydrogen Hub for the Decarbonization of a Port Industrial Area," *J. Mar. Sci. Eng.*, vol. 10, no. 2, 2022, doi: 10.3390/jmse10020231.
[70] Yang Y, et al. The scheduling of alkaline water electrolysis for hydrogen production using hybrid energy sources. Energy Convers Manag Apr. 2022;257. https://doi.org/10.1016/J.ENCONMAN.2022.115408.
[71] Fan JL, Yu P, Li K, Xu M, Zhang X. A levelized cost of hydrogen (LCOH) comparison of coal-to-hydrogen with CCS and water electrolysis powered by renewable energy in China. Energy Mar. 2022;242:123003. https://doi.org/10.1016/J.ENERGY.2021.123003.
[72] Gorre J, Ruoss F, Karjunen H, Schaffert J, Tynjälä T. Cost benefits of optimizing hydrogen storage and methanation capacities for Power-to-Gas plants in dynamic operation. Appl Energy Jan. 2020;257:113967. https://doi.org/10.1016/J.APENERGY.2019.113967.
[73] W. Cole, A. W. Frazier, and C. Augustine, "Cost Projections for Utility-Scale Battery Storage: 2021 Update," 2030, Accessed: Nov. 10, 2022. [Online]. Available: www.nrel.gov/publications.
[74] S. Kharel and B. Shabani, "Hydrogen as a Long-Term Large-Scale Energy Storage Solution to Support Renewables," *Energies 2018, Vol. 11, Page 2825*, vol. 11, no. 10, p. 2825, Oct. 2018, doi: 10.3390/EN11102825.
[75] "Future renewable energy costs: onshore wind Renewable Energies.".
[76] "GME - Statistiche - dati di sintesi MPE-MGP." https://www.mercatoelettrico.org/it/Statistiche/ME/DatiSintesi.aspx (accessed Nov. 10, 2022).
[77] International Renewable Energy Agency, *Renewable Power Generation Costs in 2021*. 2021.
[78] LevelTen, "PPA Price Index Executive Summary," 2022.
[79] European Commission, "COMMISSION DELEGATED REGULATION (EU) supplementing Directive (EU) 2018/2001 of the European Parliament and of the

Council by establishing a Union methodology setting out detailed rules for the production of renewable liquid and gaseous transport fuels of," pp. 9–25, 2022.
[80] "Terna: nel 2021 deciso recupero dei consumi elettrici +5,6% rispetto al 2020, tornati sui valori del 2019 - Terna spa." https://www.terna.it/it/media/comunicati-stampa/dettaglio/consumi-elettrici-2021 (accessed Nov. 10, 2022).
[81] I. - International Energy Agency, "Global Hydrogen Review 2022," 2022, Accessed: Nov. 10, 2022. [Online]. Available: www.iea.org/t&c/.
[82] IEA, "The Future of Hydrogen," Paris, 2019. Accessed: Nov. 14, 2022. [Online]. Available: https://www.iea.org/reports/the-future-of-hydrogen.
[83] "Nel to slash cost of electrolysers by 75%, with green hydrogen at same price as fossil H2 by 2025 | Recharge." https://www.rechargenews.com/transition/nel-to-slash-cost-of-electrolysers-by-75-with-green-hydrogen-at-same-price-as-fossil-h2-by-2025/2-1-949219 (accessed Nov. 14, 2022).
[84] IRENA, "World energy transitions outlook," *Irena*, pp. 1–54, 2022, [Online]. Available: https://irena.org/publications/2021/March/World-Energy-Transitions-Outlook.
[85] Ziegler MS, Trancik JE. Re-examining rates of lithium-ion battery technology improvement and cost decline. Cite this Energy Environ Sci 2021;14:1635. https://doi.org/10.1039/d0ee02681f.
[86] International Renewable Energy Agency, "Electricity storage and renewables: Costs and markets to 2030," *Int. Renew. Energy Agency*, no. October, p. 132, 2017, [Online]. Available: http://irena.org/publications/2017/Oct/Electricity-storage-and-renewables-costs-and-markets%0Ahttps://www.irena.org/-/media/Files/IRENA/Agency/Publication/2017/Oct/IRENA_Electricity_Storage_Costs_2017.pdf.
[87] C. Curry, "Lithium-ion Battery Costs and Market Squeezed margins seek technology improvements & new business models," 2017.